



ISLAMIC UNIVERSITY OF TECHNOLOGY
ORGANISATION OF ISLAMIC COOPERATION



**DESIGN AND ANALYSIS OF A COMPRESSED
AIR VEHICLE**

A Thesis by

Mohamoud Mohamed

Mohammad Sadeq

Kasmal Harir

Ibrahim Zakari Adimbo

BACHELOR OF SCIENCE IN MECHANICAL ENGINEERING

May (2022)

DESIGN AND ANALYSIS OF A COMPRESSED AIR VEHICLE

**MOHAMOUD MOHAMED, 151454 MOHAMMAD SADEQ,
170011077 KASMAL HARIR ,170011081 IBRAHIM
ZAKARI ADIMBO,170011082**

Submitted in Partial
Fulfillment of the
Requirements
for the Degree of

Bachelor of Science in Mechanical Engineering

**DEPARTMENT OF MECHANICAL AND PRODUCTION
ENGINEERING**

May (2022)

Certificate of Research

This thesis titled "DESIGN AND ANALYSIS OF A COMPRESSED AIR VEHICLE" submitted by Mohamoud Mohamed(151454) and Mohammad Sadeq (170011077) and Kasmal Harir (170011081) and Ibrahim Zakari Adimbo (170011082) has been accepted as satisfactory in partial fulfillment of the requirement for the Degree of Bachelor of Science in Mechanical Engineering.

Supervisor

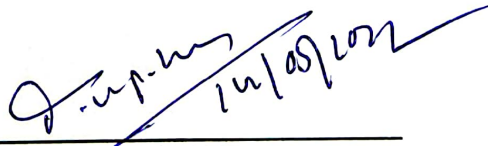


Prof. Dr. Md. Nurul Absar Chowdhury

Professor

Department of Mechanical and Production Engineering (MPE)

Head of the Department



Dr. Md. Anayet Ullah Patwari

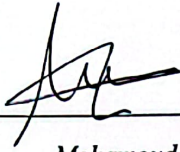
Professor

Department of Mechanical and Production Engineering (MPE)
Islamic University of Technology (IUT)

DECLARATION

I hereby declare that this thesis entitled "DESIGN AND ANALYSIS OF A COMPRESSED AIR VEHICLE" is an authentic report of our study carried out as requirement for the award of degree B.Sc. (Mechanical Engineering) at Islamic University of Technology, Gazipur, Dhaka, under the supervision of [Prof. Dr.Md. Nurul Absar Chowdhury], professor, MPE, IUT in the year 2022.

The matter embodied in this thesis has not been submitted in part or full to any other institute for award of any degree.



Mohamoud Mohamed
151454



Mohammad Sadeq
170011077



Kasmal Harir
170011081



Ibrahim Zakari Adimbo
170011082

Certificate of Research

This thesis titled “DESIGN AND ANALYSIS OF A COMPRESSED AIR VEHICLE” submitted by Mohamoud Mohamed(151454) and Mohammad Sadeq (170011077) and Kasmal Harir (170011081) and Ibrahim Zakari Adimbo (170011082) has been accepted as satisfactory in partial fulfillment of the requirement for the Degree of Bachelor of Science in Mechanical Engineering.

Supervisor

Prof. Dr. Md. Nurul Absar Chowdhury

Professor

Department of Mechanical and Production Engineering (MPE)

Head of the Department

Dr. Md. Anayet Ullah Patwari

Professor

Department of Mechanical and Production Engineering (MPE)
Islamic University of Technology (IUT)

DECLARATION

I hereby declare that this thesis entitled “DESIGN AND ANALYSIS OF A COMPRESSED AIR VEHICLE” is an authentic report of our study carried out as requirement for the award of degree B.Sc. (Mechanical Engineering) at Islamic University of Technology, Gazipur, Dhaka, under the supervision of [Prof. Dr.Md. Nurul Absar Chowdhury], professor, MPE, IUT in the year 2022.

The matter embodied in this thesis has not been submitted in part or full to any other institute for award of any degree.

*Mohamoud Mohamed
151454*

*Mohammad Sadeq
170011077*

*Kasmal Harir
170011081*

*Ibrahim Zakari Adimbo
170011082*

ACKNOWLEDGEMENT

First and foremost, we feel grateful and acknowledge our profound indebtedness to Prof. Dr. Md. Nurul Absar Chowdhury, Professor, Department of Mechanical and Chemical Engineering, IUT. His endless patience, scholarly guidance, continual encouragement, constant and energetic supervision, constructive criticism, valuable advice at all stage has made it possible to complete this project. We would also like to offer thanks to all friends who make this a successful project. We acknowledge our sincere indebtedness and gratitude to our parents for their love, support and the efforts they have done for us so far.

We seek excuse for any errors that might be in this report despite of our best efforts.

ABSTRACT

Global climate change is the most pressing issue facing the entire globe. Vehicles are one of the primary contributors of pollution. As a result, non-conventional fuels must be substituted for conventional fuels. Compressed air is one such alternate fuel. This is a clean, simple, and safe fuel that has no negative impact on the environment. The purpose of this research is to investigate compressed air as a vehicle fuel. A compressor fills compressed air with electrical energy. When calculating total efficiency, the electricity required to compress air must be taken into account. The air engine is now the most often utilized mechanism for converting compressed air potential energy into mechanical energy. Nonetheless, the compressed air vehicle will help to reduce air pollution and eventually reach zero, as well as promote a healthy environment. There is no combustion taking place there. Light utility vehicles are gradually gaining popularity as a means of short-distance mobility. With each passing decade, the information on air quality allows for continuously improving decisions that have led to a much cleaner atmosphere by making pollution sources of earlier decades become obsolete. The current fossil fuel energy sources are rapidly depleting and their combustion products contribute to the major environmental and health problems. It is, therefore, necessary to look for adopting renewable sources of energy as an alternative which in turn reduces pollution and avoids the consumption of nonrenewable fuel sources. This project shows a prototype design of a vehicle that uses compressed air as a source of power to move. The atmospheric air is compressed to very high pressure and sent to the engine for power production. The car's components are designed and their properties are provided using Solid works design and simulation. Some of the part's dimensions and parameters are calculated by hand calculation. In the later part of this project, research has been done on how the actual compressed air vehicles were effective so far, the recent development of this system, and how can we make the technology more compact and efficient.

Keywords: compressed air vehicle, solid work simulation, engine, Alternative source of energy, non pollutant

Table of Contents

Certificate of Research	iii
DECLARATION	iv
ACKNOWLEDGEMENT	v
ABSTRACT	vi
LIST OF FIGURES	viii
LIST OF TABLES	x
Nomenclature	xi
CHAPTER ONE INTRODUCTION	1
1.1 Problem statement	1
1.3 Purpose and significance of the thesis	12
CHAPTER TWO LITRATURE REVIEW	13
2.1 The Technology of Compressed Air Engine	13
2.2 Development of Compressed Air Engine	14
2.3 Advantages of Compressed Air vehicles	15
2.4 Drawback of compressed Air Engines	16
CHAPTER THREE METHODOLOGY	17
3.1 The Pneumatic setup.....	17
3.2 The control unit	18
3.3 The crankshaft design.....	30
3.4 Connecting rod design	41
3.5 Chassis design	52
3.6 Differentials.....	57
3.7 bearings design.....	61
CHAPTER FOUR RACENT ADVANCEMENTS	63
4.1 Technology Air Storage & Refueling.....	63
4.2 Input Energy	63
4.3 Temperature Control	63
4.4 Multistage Compression	63
4.5 FUTURE SCOPE	64
CHAPTER FIVE RECENT STUDIES	65
CHAPTER SIX RESULT AND DISCUSSION	69
6.1 Analysis	69
CONCLUSION	71
References	72

LIST OF FIGURES

Figure 1: compressed air vehicle model	14
Figure 2: Final design of the project.....	17
Fig 3.2: Figure 3The pneumatic setup	18
Figure 4:nrf24l01 wireless module pinout.....	19
Figure 5: TIP120 Darlington transistor pinout	19
Figure 6: Arduino Uno R3.....	19
Figure 7: breadboard.....	19
Figure 8: The transmitter circuit.....	20
Figure 9 :the transmitter circuit diagram	20
Figure 10: the receiver circuit.....	21
Figure 11: the receiver circuit diagram.....	21
Figure 12: The code used to program the Arduino UNO R3 in the transmitter circuit.....	22
Figure 13: The code used to program the Arduino UNO R3 in the receiver circuit	23
Figure 14: the steering mechanism	24
Figure 15:pivoted hinge.....	25
Figure 16: Servo motor construction	
Figure 17 :Servo motor pinout.....	25
Figure 18: joystick	26
Figure 19: The transmitter circuit for the steering system.....	26
Figure 20: The receiver circuit for the steering system	27
Figure 21: The Arduino code for the transmitting circuit in the steering system.....	28
Figure 22: The Arduino code for the receiver circuit in the steering system	29
Figure 23:Crank shaft geometry after mesh	42
Figure 24: Boundary conditions of the simulation	42
Figure 25: the stresses acting on the crankshaft	42
Figure 26:The deformation of the crankshaft	43
Figure 27: The strain of the crankshaft.....	43
Figure 28: Connecting rod.....	41
Figure 29: The cross-section of a connecting rod.....	41
Figure 30:typical dimensions of the connecting rod at the middle.....	42
Figure 31:The big end of the connecting rod	
Figure 32: The small end of the connecting rod.....	45
Figure 33: The model after mesh is generated	
Figure 34: A model of the connecting rod.....	50
Figure 35 :the boundary condition defined on the connecting rod.....	51
Figure 36: stresses on the connecting rod.....	52
Figure 37: deformation of the connecting rod.....	51
Figure 38: strain of the connecting rod.....	52
Figure 39: Top view of the chassis.....	53
Figure 40 : Isometric view of the bar holing the pneumatic actuators	53
Figure 41: Top view of the bar holing the pneumatic actuators	54
Figure 42: a model of the beam carrying the maximum load after mesh generation	55
Figure 43:The boundary conditions applied to the beam carrying the maximum load.....	55
Figure 44: The stresses on the beam carrying the maximum load	56
Figure 45: The deformation of the beam carrying the maximum load.....	56
Figure 46: The strain of the beam carrying the maximum load	57

Figure 47: The differentials assembly	57
Figure 48: construction of ball bearings	61
Figure 49: Dimensions of the ball bearing	62

LIST OF TABLES

Table 1: the mechanical properties of AISI 1045.-----	41
Table 2: the mechanical properties of AISI 1045.-----	49
Table 3: properties of the chassis material -----	54
Table 4: Running the engine on compressed air keeping the Pressure constant -----	69
Table 5: Running the engine on 160 liters capacity compressed air filled cylinder and note its time duration at different pressure. -----	69

Nomenclature

PCV	Positive crankcase ventilation
NO	nitric oxide
NO ₂	nitrogen dioxide
N ₂ O	nitrous oxide
NO ₃	nitrate ion
N ₂ O ₃	dinitrogen trioxide
N ₂ O ₄	dinitrogen tetroxide
N ₂ O ₅	dinitrogen pentoxide
COPD	chronic obstructive pulmonary disease
CO	carbon monoxide
COHB	carboxyhemoglobin
EGR	Exhaust gas recirculation
LUV	light utility vehicles
ZPM	Zero Pollution Motors
RF	radio frequency
MDI	Multi-Device Interface

CHAPTER ONE INTRODUCTION

1.1 Problem statement

The exhausted gas from the vehicle contains a lot of harmful chemical compounds. The presence of these contaminants has a deleterious impact on human health, welfare and the environment. These pollutant substances are considered to be responsible for the photochemical smog, acid rain, a reduced atmospheric visibility and the global warming. Air pollution has been recognized as a very complex societal problem where its cause and effect relationships have been reasonably deductive.

The major cause of the air pollution is combustion. When it occurs, the hydrogen and carbon from the fuel reacts with the oxygen in the air producing heat, light, carbon dioxide and water vapor. Some side products of this reaction such as nitrogen oxides, carbon monoxide, sulfur oxides, fly ash and hydrocarbons are formed due to impurities in the fuel, poor fuel-to-air ratio, too high or too low combustion temperature. These chemical compounds are air pollutants.

The industrial revolution had the abundant share of polluting the air. Burning the coal for the factories and power generation was a major source of the chemical pollutant of the atmosphere. Which appears as smog (smoke and fog) in the air.

A similar air condition was reported in 1995 in the United States. The national air quality standards for specific air pollutants were violated in several regions and areas. These locations included 77 areas for ozone, 36 for carbon monoxide, 82 for particulate matter, 43 for sulfur dioxide, 11 for lead and one for nitrogen dioxide.

The air pollution used to be an intractable issue for most of the world before the 20th century. In 1200s, King Edward I of England tried to find a solution for the polluted atmosphere of London by banning the use of sea coal. King Edward II ordered the execution of anyone found burning coal while the British Parliament was meeting. Starting from the authority of Richard II (1377 -1399) and later under Henry V (1413-1422), England began to issue policies to regulate the use of coal in order to reduce the emissions affecting the air quality.

With each passing decade, the information on air quality allows for continuously improving decisions that have led to a much cleaner atmosphere by making pollution sources of earlier decades become obsolete and are replaced by processes and equipment that produce less pollution. The improvement has been remarkable, mainly in the health-related criteria air pollution.

Since 90% of the emissions are gases, the suitable solution seems to reduce the amount of the harmful gaseous particles from the effluent gas. Several ways have been developed and

improved to treat the exhausted gases after the combustion. One of them is to adsorb the pollutant species on the surface of a solid adsorbent based on the ability of some solids to remove components from a flow stream using Van Der Waals force of attraction. Another method to reduce the impurities in the air flow is absorption of the species in a liquid solvent where the dirty effluent gas is brought in contact with a scrubbing liquid. The contaminated gas is absorbed in the liquid then the contaminated liquid is changed. The pollutant might also be oxidized by combusting the flue gas by means of direct flame or catalytic incineration to alter the reaction products to other forms which are not pollutant. The last approach to control the contaminated exhaust gas is to reduce the concentration of the diluents from the fuel or the oxidant using filters.

The first effort at controlling pollution from automobiles was the positive crankcase ventilation (PCV) system. This draws crankcase fumes heavy in unburned hydrocarbons a precursor to photochemical smog into the engine's intake tract so they are burned rather than released them to the atmosphere. Positive crankcase ventilation was first installed on a widespread basis by law on all new 1961-model cars first sold in California, USA. The following year, New York required it. By 1964, most new cars sold in the U.S. were so equipped, and PCV quickly became standard equipment on all vehicles worldwide.

1.1.1 Vehicle emissions and their impact on human health

The composition of the exhaust emissions varies depending on air-to-fuel ratio, speed, combustion efficiency, and the fuel purity. However, there are some contaminants usually present in the flue gas; such as hydrocarbons, nitrogen oxides, carbon monoxide, carbon dioxide, photochemical oxidants, particulate matter, and sulfur oxide. These pollutants affect negatively the human health and the environment.

Effect of hydrocarbons, nitrogen oxides and photochemical oxidants on human health

The emission of hydrocarbons is related to the combustion efficiency. That occurs when unburned fuel vaporizes and leave the combustion chamber with the exhaust gas. Though the hydrocarbons are not considered as pollutants as a general list, a huge number of specific hydrocarbons are identified as hazardous pollutants and studies of certain hydrocarbons classes found them responsible for some types of cancer.

The atmospheric air contains nitrogen oxides in different forms. These include nitric oxide (NO), nitrogen dioxide (NO₂), nitrous oxide (N₂O), nitrate ion (NO₃), dinitrogen trioxide (N₂O₃), dinitrogen tetroxide (N₂O₄) and dinitrogen pentoxide (N₂O₅). The Nitric Oxide (NO) and Nitrogen dioxide (NO₂) are usually referred by the term nitrogen oxides (NO_x). The exposure to NO₂ was found to be a reason to chronic obstructive pulmonary disease (COPD).

The combination of hydrocarbons and nitrogen oxides in presence of the sunlight form photochemical oxidants including ozone (O₃) which affects the human health. The photochemical oxidants refer to the oxidizing agents that can oxidize the potassium

iodide, eg, peroxyacetyl nitrate, Formic acid, hydrogen peroxide. These oxidants affect the well-being of human by causing severe eye, nose and throat irritation, chest constriction and severe coughing and inability to concentrate at high concentrations.

Effect of carbon monoxide on human health

As a source of the hydrocarbons, the exhausted unburned fuel also contains carbon monoxide (CO) which can stay in the atmosphere up to 4 months. During the period of 1970 to 1980 in the U.S., about 70% of the carbon monoxide emissions were from the highway vehicles. Although a small amount of carbon monoxide is discharged from a vehicle due to the emission control systems, the danger presents from the number of vehicles available on the road and the distance the travel.

Besides participating in the photochemical reactions, the carbon monoxide causes physiological and pathological changes and toxic inhalant that prevent the body tissues from necessary oxygen.

The carbon monoxide is a direct motive of the carboxyhemoglobin (COHB) when it combines with the hemoglobin which leads to oxygen deficiency in the body.

Effect of particulate matter on human health

The term particulate matter refers to the solid or liquid particles larger than $0.0002\ \mu\text{m}$ but less than $500\ \mu\text{m}$ in diameter. 20 to 60% of the emitted particles are between 0.01 and $2.5\ \mu\text{m}$. Inhaling these particulate matters alone or combined with other pollutants can severely damage the respiratory organs after they are deposited in the lungs. The danger of the particulate matters is subjected to their inherent chemical or physical characteristics and it might as well obstruct one or more mechanisms which normally clears the respiratory tract in addition to ability of the liquid particulates to absorb toxic matters or adsorb them in case of solid particles.

Effect of sulfur oxides on human health

The sulfur dioxide and trioxide have the highest concentrations in the atmosphere among all sulfur oxides. The combination of sulfur oxides with particulate matters and moisture forms a serious health hazard.

Bronchoconstriction is a result from the exposure to sulfur dioxide which is a condition when the smooth muscles of the bronchus contracts. This muscle contraction causes the bronchus to narrow and restrict the amount of air passing into and out of the lungs.

1.1.2 Vehicle emissions and their impact on environment

Along with harming human health, air pollution can cause a variety of environmental effects:

Acid rain

Acid rain is defined as the wet and dry deposition of acidic substances from the atmosphere. These acids fall to earth in form of rain, snow, cloud water droplets, or solid particles. These acids are formed from nitrogen oxides and sulfur oxides exhausted to the atmosphere after the combustion of fuel. The danger of acid rain is it damages trees and causes soils and water bodies to acidify, making the water unsuitable for some fish and other wildlife.

Ozone depletion

Ozone (O₃) is normally present at the stratosphere (Earth's upper atmosphere). It forms a layer that protects life on earth from the sun's harmful ultraviolet (UV) rays. However, its presence at ground level is considered harmful. Thinning of the protective ozone layer increases the amounts of UV radiation that reaches the Earth. UV can also damage sensitive crops, such as soybeans, and reduce crop yields. The ozone depletion is caused by the nitric oxide (NO).

Global warming and climate change

The Earth's atmosphere temperature is balanced naturally by receiving heat from sun and releasing infrared radiation that sends heat back into space. This "greenhouse effect" keeps the Earth's temperature stable. The increasing concentration of carbon dioxide CO₂ limits the travel of the infrared radiation as CO₂ absorbs infrared. As a result, the temperature of the Earth is increasing, resulting in the melting of ice, icebergs, and glacier. Many scientists believe that global warming could have significant impacts on human health, agriculture, water resources, forests, wildlife, and coastal areas.

1.2 emissions control in engines

Since recognizing the major effects of car emissions on the air pollution, a lot of method, techniques and engine modifications have been developed to reduce the amount of pollutants that vehicles engine produce.

1.2.1 Catalytic convertor

One way to control the engine emissions is to provide more area for the combustion to occur. The additional space is called catalytic convertor. This convertor is placed in the exhaust system and platinum or palladium shaped like honeycomb is used as catalysts to speed up the reactions. When carbon monoxide or hydrocarbons pass over the catalyst, they are oxidized to carbon dioxide and water vapor.

This process generates heat proportionally related to the dirtiness of the exhaust gas. So, in extreme conditions, the heat generated might destroy the catalytic convertor.

1.2.2 Exhaust gas recirculation (EGR) valve

The nitrogen oxides are produced when the temperature in the combustion chamber is excessively high. The EGR valve is used to redirect a limited amount of the exhaust gas back to the intake system to dilute the air-fuel mixture. This process has an adverse impact on the efficiency of the engine. EGR valve does not take any action when the engine starts and when full engine power is needed.

1.2.3 Evaporative control system

The evaporative control system is used to trap the fuel vapor from the fuel tank and the carburetor due to the nature of fuel. The fuel vapor is collected in charcoal canister then drawn to the engine when it starts to be burned with the fuel-air mixture.

The fuel vapor is sent to the intake system with the help of the engine vacuum. A purge valve is used to regulate the vapor flow into the engine.

The drawback of this system that the purge valve fails and the vapors will go directly to the intake system unregulated.

1.2.4 Air injection

The air injection system was developed to completely burn the unburned fuel particles in the exhaust flow which is a primary source of the hydrocarbons. Introducing oxygen to the heat and unburned fuel in the exhaust manifold ignites these fuel particles.

1.2.5 Engine modifications

In addition to the separated emission control systems, some improvements can be implemented to the engine to reduce the amount of produced pollutants. However, these modifications depend on the engine type.

For SI engines, the carburetor can be completely replaced by multi-port fuel injection system. The fuel supply to the cylinder can be accurately regulated using electronic engine management by sensing different engine parameters. The combustion chamber design can also be improved by replacing the 2-valve system with 4-valve system.

Using ceramics components such as piston pin, valves and blades in turbochargers has a significant impact on the pollutant's emission. The turbo-compounded engine are found to be up to 18% better than the conventional engines.

On the other hand, the major pollutants from CI engine can be reduced as follows; Hydrocarbons emission control requires low-sac nozzle to improve the combustion. The nitrogen dioxides emission control is assisted by cooling the intake air before entering the engine resulting in retarded combustion. Finally, the particulate emissions control is associated with high injection pressure for a fine fuel atomization.

1.3 Purpose and significance of the thesis

All mentioned methods of controlling the contaminations in a gas flow are not 100% efficient. So from our point of view, the ideal solution for the air pollution caused by the vehicles emissions is to eliminate the pollutant in the first place by utilizing the clean renewable energy sources to power the cars. Hence, we are designing a prototype of a vehicle that exploit the compressed natural air to push the pistons in the engine instead of combusting fuel. The purpose is to have a closer look on an engine with zero emission using the renewable energy with the minimum operating cost.

CHAPTER TWO LITRATURE REVIEW

Because we live in such a mobile world, light utility vehicles (LUVs) such as bicycles and cars are becoming increasingly popular modes of short-distance independent transportation. Petrol and diesel, which have long been the primary sources of transportation fuel, are becoming increasingly expensive and impractical (especially from an environmental standpoint). As a result of these issues, vehicle makers are developing alternative-energy vehicles. When fuel-free flying (like birds), i.e., flying based on the use of bio-energy and air power in the atmosphere, appears to be nearly impossible for humans at this point in technological development, engineers are fascinated at least by the enormous power associated with the human-friendly and tried source of energy (i.e., air) to develop air-powered vehicles as an alternative. Engineers are directing their true endeavors to use air as a fuel source to run LUVs, which will allow future bicycles and light/small vehicles to run on air power for daily schedule distances, making mobility free of contamination and practicable.

2.1 The Technology of Compressed Air Engine

Windmills, sails, balloon cars, hot air balloon flying, hang gliding, and other applications of uncompressed air power have been used by mankind for ages. The use of compressed air for energy storage [3] is a method that is not only efficient and clean, but also cost-effective, and has been utilized to power mine trains and naval torpedo propulsion since the 19th century. The London-based Liquid Air Company began producing compressed air and liquified air cars in 1903. The lack of force delivered by the "motors" and the cost of packing the air were major issues with compacted air vehicles. As of late a few organizations have begun to create compacted air vehicles, albeit none has been delivered to the public up until now. Com-squeezed air tanks store power truly well however are missing on force thickness. They tie or beat batteries in the charge/re-charge proficiency and thoroughly execute them on life expectancy. Higher pressing factors are their huge issue of compacted air vehicles while productivity, cost, poisonous synthetics, and life expectancy are the enormous issues related with substance batteries. The rule of compacted air drive is to pressurize the capacity tank and afterward interface it to something exceptionally like a responding

The vehicle's steam engine. Packed air vehicles (CAV) use the development of compressed air to drive their cylinders instead of combining fuel with air and consuming it in the engine to drive cylinders with hot extending gases. As a result, the innovation is free of the technical and clinical issues associated with using alkali, petroleum, or carbon disulphide as the working liquid. Makers [5-9] claim to have a 90 percent effective designed motor. The air is compressed at a pressure that is several times that of the air pumped into vehicle tires or bicycle tires. The tanks should be designed to meet the safety requirements of a pressing factor vessel. Steel, aluminum, carbon fiber, Kevlar, or other materials, or combinations of the aforementioned, could be used to construct the capacity tank. Although fiber materials are lighter than metals, they are frequently more expensive. Metal tanks can endure a lot of pressing factor cycles, but they should be examined for erosion every now and again. An organization has expressed interest in storing air in tanks with a pressure of 4,500 pounds per square inch (about 30 MPa) and a capacity of nearly 3,200 cubic feet (roughly 90 cubic meters). The tanks could be topped off at an assistance station with heat exchangers, or at home or in parking lots in a couple of hours by connecting the vehicle to an on-board blower.

2.2 Development of Compressed Air Engine

Jem Stansfield, an English inventor has been able to convert a regular scooter to a compressed air moped shown in Fig2.1 This has been finished by furnishing the bike with a packed air motor and air tank. Jem Stansfield made the bicycle by strong two high-pressure tanks onto the side of his Puch sulked the tanks are fundamentally scuba tanks. He utilizes the power from his home to fill the tanks



Fig 2.1: compressed air vehicle model

The force is then "put away" there, similar as a battery, prepared for use. The tanks utilized are carbon-fiber tanks of the sort utilized by firemen for oxygen. Yet at the same time, they're far less expensive than even the lead corrosive battery utilized in vehicle now. Obviously, the blower chips away at power, so that is not generally a spotless force source but rather re-energizing choices

around evening time or off pinnacle will upgrade the odds to utilize the force that would be squandered something else. The maximum velocity is around 18 mph, and it can just go 7 miles before the pneumatic force runs out and significantly more force could most likely be pulled by tweaking his setup. A little stuff on the finish of the air drill, associated with the chain of the bicycle would make a significantly richer arrangement. A few organizations are exploring and creating models, and others intend to offer air fueled vehicles, transports and trucks. The compacted air is put away in carbon-fiber tanks that are incorporated into the frame. As the air is delivered, the pressing factor drives cylinders that power the motor and move the vehicle, and the cylinders pack the air into a repository so the cycle proceeds. In the wake of making an unrest by delivering the world's least expensive vehicle Tata nano, India's biggest automaker (Tata Motors) is set to begin creating the world's first business air-controlled vehicle. The "Air Car" will propel its motor's cylinders with compressed air rather than gas and oxygen blasts like inside ignition vehicles. By 2010, Zero Pollution Motors (ZPM) (USA) plans to produce the world's first air-fueled vehicle for the US market. An previous version of the automobile is noisy, slow, and a tad clunky, but this vehicle will not be competing with Ferrari or Rolls-Royce, and the manufacturers have no plans to produce a Formula One version. The target market for air-powered cars is the urban motorist, including delivery vehicles, taxi drivers, and people who merely want to go to the store. The most recent air car is believed to have improved dramatically over the previous model. It is supposed to be significantly quieter, with a top speed of 110 km/h (65 mph) and a range of roughly 200 kilometers before requiring air filling.

2.3 Advantages of Compressed Air vehicles

In comparison to petrol or diesel powered vehicles “air powered vehicles” have the following advantages:

- Air, all alone, is non-combustible, plentiful, prudent, movable, storable, and above all, nonpolluting.
- Because no cooling system, fuel tank, spark plugs, or silencers are required, compressed air technology saves vehicle production costs by around 20%.
- High torque in a small package.
- The engine's mechanical design is simple and reliable.
- Low production and maintenance costs, as well as simple upkeep.

2.4 Drawback of compressed Air Engines

- Because compressed-air vehicles are still in the pre-production stage and have not been widely examined by independent observers, their disadvantages are less well understood. Some technological obstacles can be summarized as follows:
- Compressed air vehicles probably will be less powerful than common vehicles of today. Which represents a peril to clients of packed air vehicles imparting the way to bigger, heavier and more inflexible vehicles
- At the point when the air is extended in the motor, it will chill off through adiabatic cooling and lose constrain in this way its capacity to take care of job at colder temperatures. It is hard to keep up or reestablish the air temperature by basically utilizing a heat exchanger with surrounding heat at the high stream rates utilized in a vehicle, subsequently the ideal isothermic energy limit of the tank won't be figured it out. Cold temperatures will likewise urge the motor to ice up.

CHAPTER THREE METHODOLOGY

The researches about the air compressed engines are rapidly progressing to provide a modern way to run the vehicles without the use of the combustion.

The air is drawn from the atmosphere and stored in tanks using a compressor. To power the vehicle, some air is released to the expansion chamber -equivalent to combustion chamber- where it pushes the piston downward generating the reciprocating motion which is then converted to rotary motion with the help of the crank shaft and connecting rod. To control the air flow from the tanks to the expansion chamber, a high speed shutter is used.

The same working principle is used in this project where the high speed shutter is replaced by 4 ways 5 ports solenoid valve and a pneumatic actuator takes the place of the cylinder and piston assembly.

3.1 The Pneumatic setup

Figure 3.1 shows the final result of this project. As illustrated in the figure 3.2; through a manifold, a compressor quick release fitting, pressure gauge, safety relief valve, and ball valve are connected directly to the air cylinder. The air flows from the cylinder toward the 5-Ports 4-Ways solenoid valve through a pressure regulator to maintain a safe operating pressure in the solenoid valve and the pneumatic cylinder (140 PSI) and a ball valve to cut the air flow to the actuator.

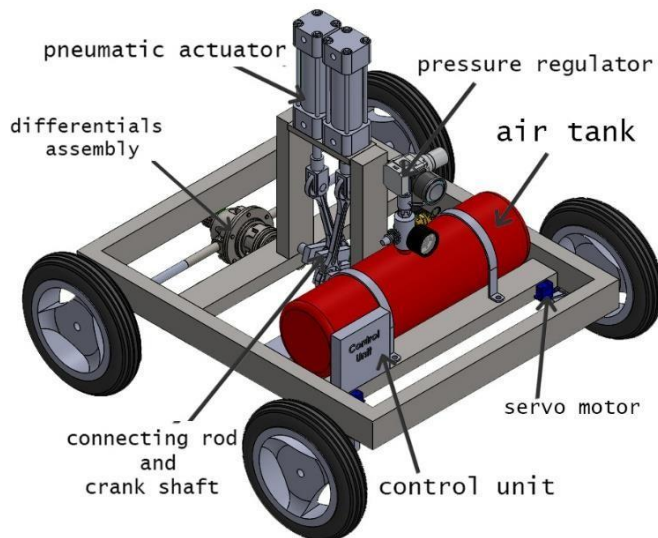


Fig 3.1: Final design of the project

The 5-Ports, 4-Ways solenoid valve is directly linked to the pneumatic cylinder and two flow control mufflers are associated with the solenoid valve to control the speed of the actuator's rod extending and retracting. The 5-Ports, 4-Ways solenoid valve is directly linked to the pneumatic cylinder and two flow control mufflers are associated with the solenoid valve to control the speed of the actuator's rod extending and retracting. The solenoid valve is connected to the control unit in order to control the operation of the pneumatic actuator. While the safety relief valve is used to evacuate the air cylinder.

The compressor quick release fitting is used to easily and quickly connect the compressor to the air cylinder for the refill.

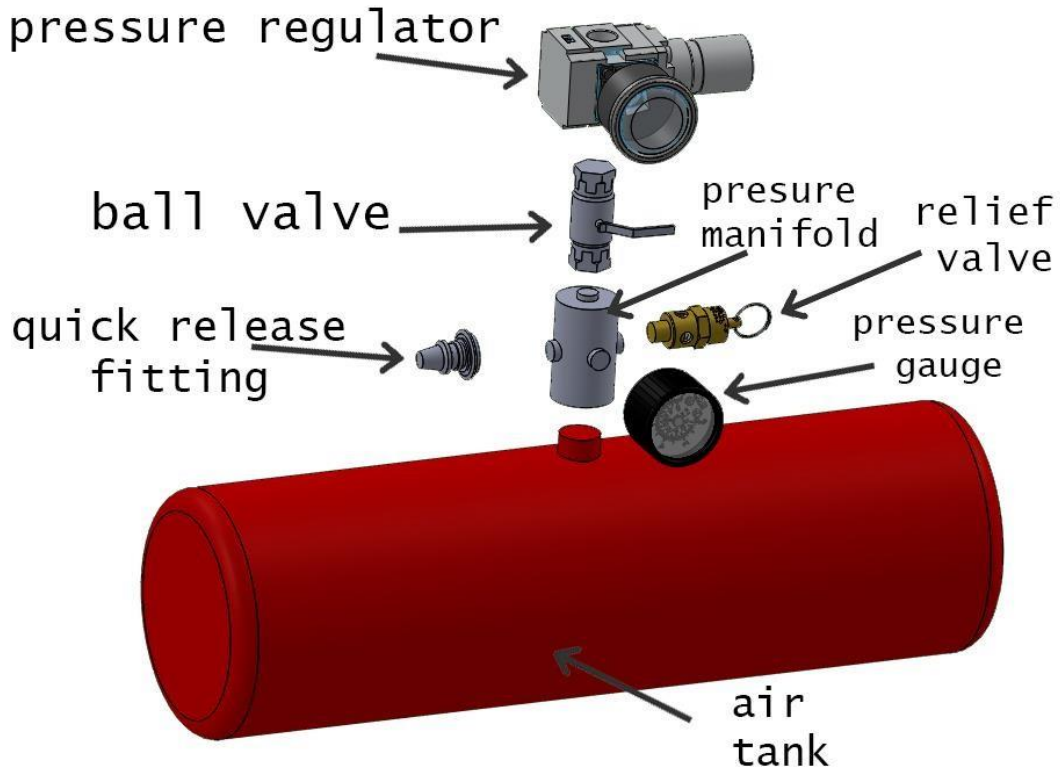


Fig 3.2: The pneumatic setup

3.2 The control unit

The control unit contains the receiver circuits to manage the operation of the 4 ways 5 ports solenoid valve and the steering system.

3.2.1 Controlling the 4 ways 5 ports solenoid valve

In order to control the solenoid valve, the following components are needed. 2 pieces of nrf24l01 2.4GHz wireless module, 9V toggle switch, two 10k Ω resistors, TIP120 Darlington Transistor, Rectifier diode (1N4001), 9 & 12V power sources, and two Arduino UNO R3 in addition to breadboards.

The following pictures show the different components needed in the circuits.

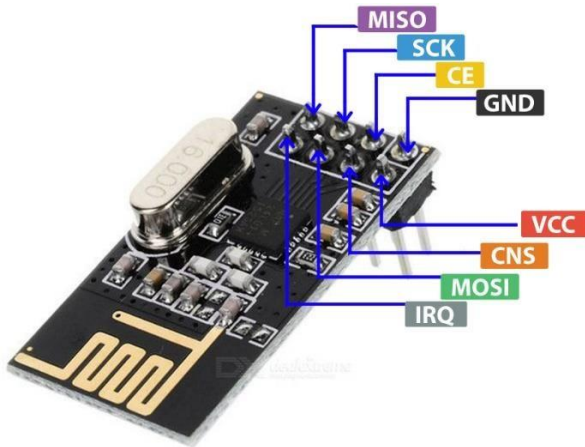


Fig 3.3: nrf24l01 wireless module pinout

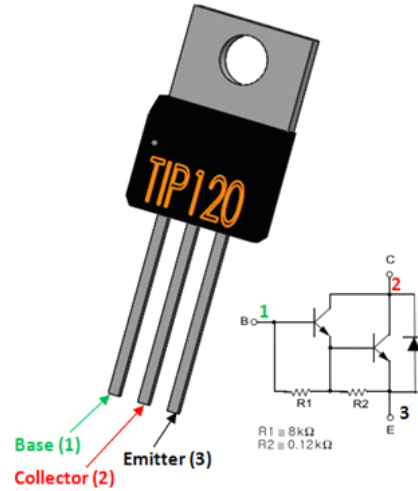


Fig 3.4: TIP120 Darlington transistor pinout

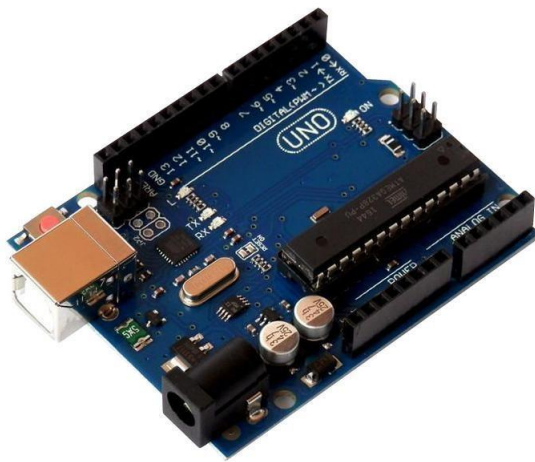


Fig 3.5: Arduino Uno R3

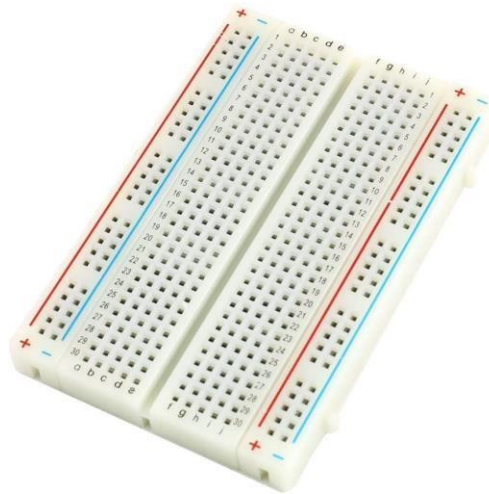


Fig 3.6: breadboard

To move the vehicle, the pneumatic actuator is remotely triggered using two Arduino circuits. The transmitter circuit initiates RF contact with the receiver circuit and sends it a message when the toggle switch is on. Wiring the nrf24l01 is the same in both transmitter and receiver circuits. However, the receiver Arduino circuit receives a signal performs an action which is to switch on the solenoid valve using the TIP120 Darlington transistor which allows 12V toward the solenoid once a signal is received from the transmitter circuit. Two pull-down resistor ($10k\Omega$) are used as a protection for the Arduino Unos from the high voltage. The Rectifier diode (1N4001) is required for the solenoid to prevent transient voltage from flowing through the system caused when a magnetic coil suddenly loses power once the solenoid is fired.

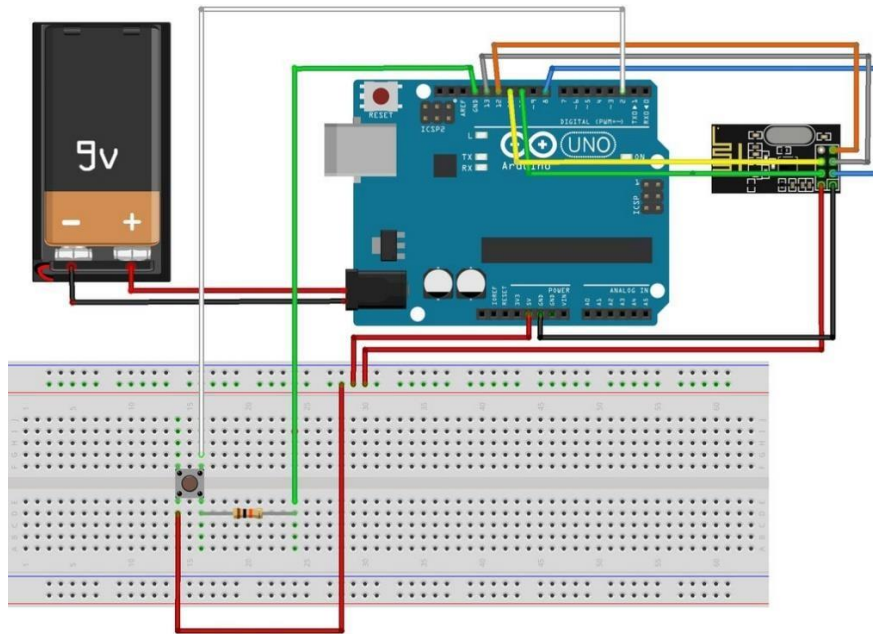


Fig 3.7: The transmitter circuit

The figure above shows the connection of the transmitter circuit used in controlling the 4 ways 5 ports solenoid valve. Here, 9V source is used to power the Arduino UNO R3 and one nrf24101 wireless module is used. The Arduino UNO R3 is programmed in such a way when the toggle switch is pushed, it sends signal to the nrf24101 wireless module which generates a radio frequency (RF) wave. The other Arduino UNO R3 in the receiver circuit is programmed so the nrf24101 wireless module works as a receiver. When the wireless module reads the RF wave, it sends signal to the TIP120 Darlington transistor allowing 12V to the solenoid. Figure 3.8 shows the circuit diagram of the transmitter circuit.

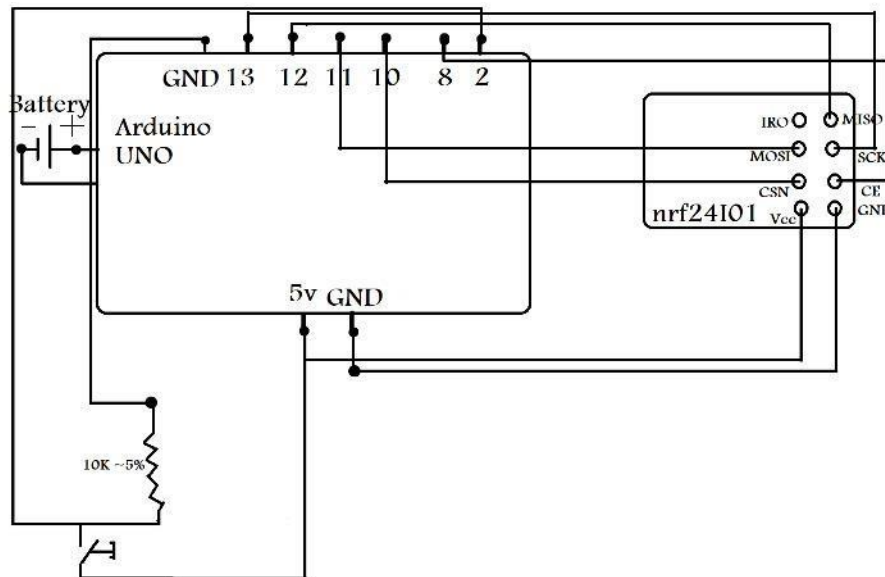


Fig 3.8: the transmitter circuit diagram

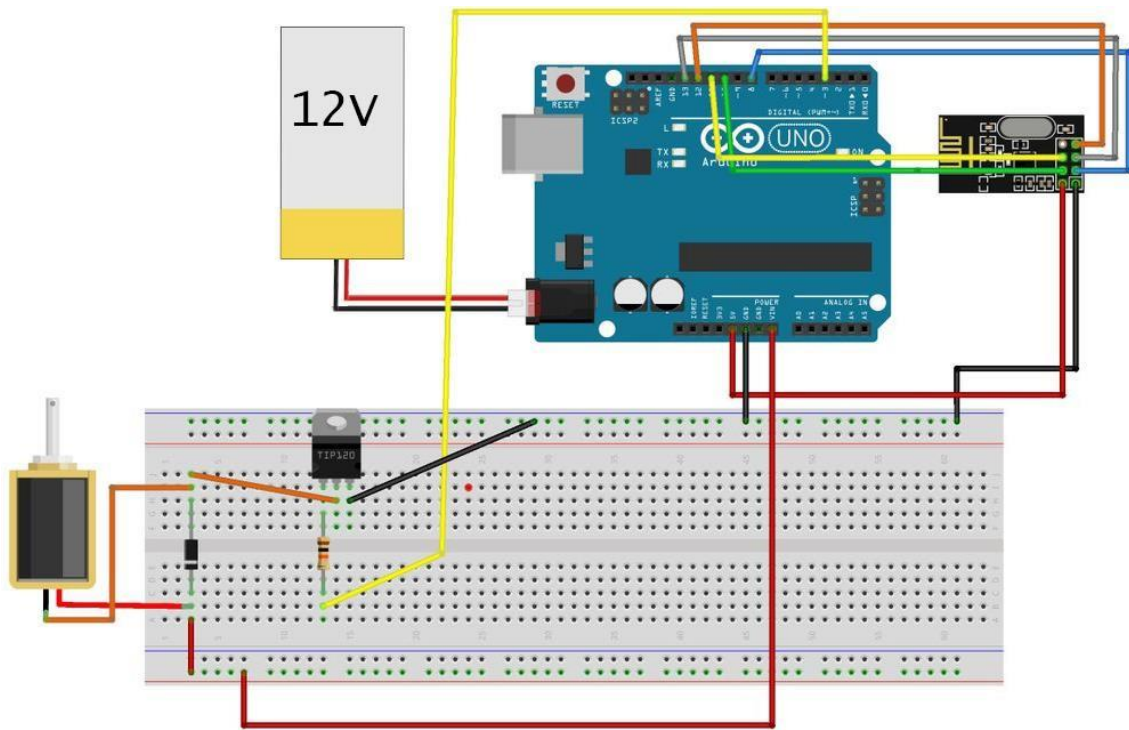


Fig 3.9: the receiver circuit

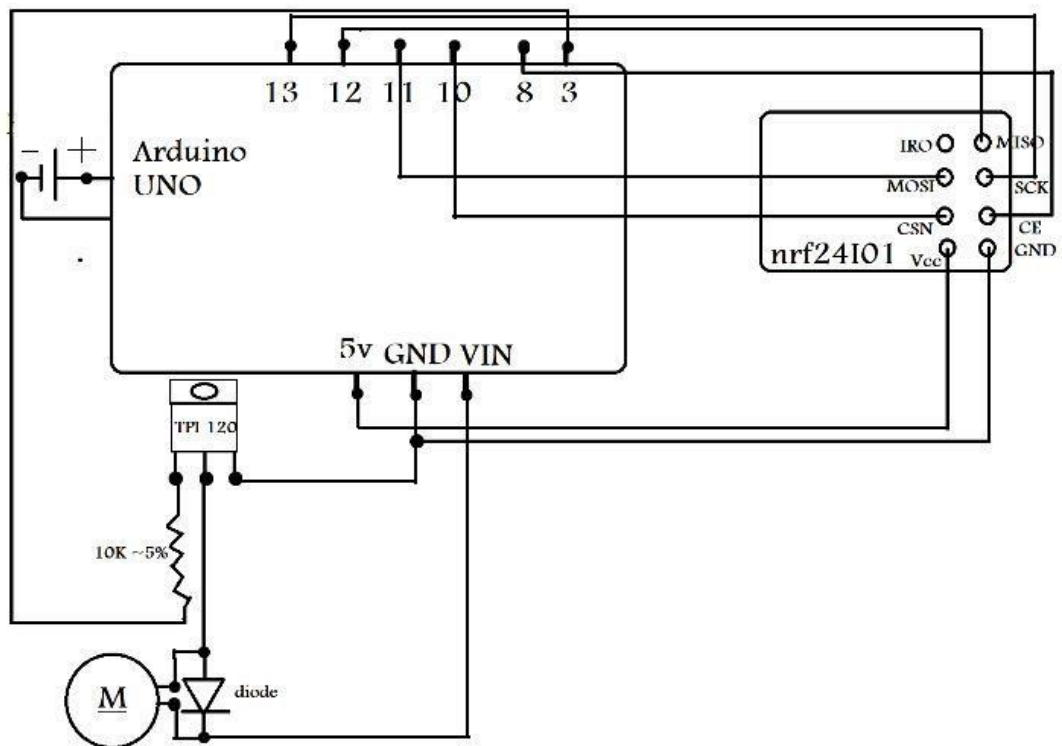


Fig 3.8: the receiver circuit diagram

```
sketch_feb23a $  
  
/*  
NRF24L01      Arduino  
CE           >   D8  
CSN          >   D10  
SCK          >   D13  
MO           >   D11  
MI           >   D12  
RO           >   Not used  
GND          >   GND  
VCC          >   5V  
*/  
#include <SPI.h>  
#include <RH_NRF24.h>  
const int button = 2;  
  
void setup()  
{  
  Serial.begin(9600);  
  if (!nrf24.init())  
    Serial.println("init failed");  
  // Defaults after init are 2.402 GHz (channel 2), 2Mbps, 0dBm  
  if (!nrf24.setChannel(125))  
    Serial.println("setChannel failed");  
  if (!nrf24.setRF(RH_NRF24::DataRate2Mbps, RH_NRF24::TransmitPower0dBm))  
    Serial.println("setRF failed");  
}  
void loop()  
{  
  if (digitalRead(button) == HIGH)  
  {  
    uint8_t data[] = "104";  
    nrf24.send(data, sizeof(data));  
  }  
  delay(50);  
}
```

Fig 3.9: The code used to program the Arduino UNO R3 in the transmitter circuit

```
sketch_feb23a $
/*
NRF24L01      Arduino
CE            >    D8
CSN          >    D10
SCK          >    D13
MO           >    D11
MI           >    D12
RO           >    Not used
GND          >    GND
VCC          >    5V
*/
#include <SPI.h>
#include <RH_NRF24.h>
const int FIRE = 3;
int timeOUT = 0;
RH_NRF24 nrf24;
void setup()
{
  pinMode(FIRE, OUTPUT);
  Serial.begin(9600);
  if (!nrf24.init())
    Serial.println("init failed");
  if (!nrf24.setChannel(125))
    Serial.println("setChannel failed");
  if (!nrf24.setRF(RH_NRF24::DataRate2Mbps, RH_NRF24::TransmitPower0dBm))
    Serial.println("setRF failed");
}
void loop()
{
  if (nrf24.available())
  {
    uint8_t buf[RH_NRF24_MAX_MESSAGE_LEN];
    uint8_t len = sizeof(buf);
    if (nrf24.recv(buf, slen)
        {
          Serial.print("got request: ");
          Serial.println((char*)buf);
          int sig = atoi((const char*) buf);
          if (sig == 104)
          {
            digitalWrite(FIRE, HIGH);
            timeOUT = 0;
            delay(150);
            digitalWrite(FIRE, LOW);
          }
        }
    else {
      if (timeOUT > 1000)
      {
        digitalWrite(FIRE, LOW);
      }
      timeOUT++;
    }
  }
}
```

Fig 3.9: The code used to program the Arduino UNO R3 in the receiver circuit

3.2.2 The steering system control

The steering mechanism rely on attaching the wheel shaft on a pivoted hinge. A servo motor with the help of a connecting rod pushes and pulls the hinge to change its angle to result in the vehicle's rotation.

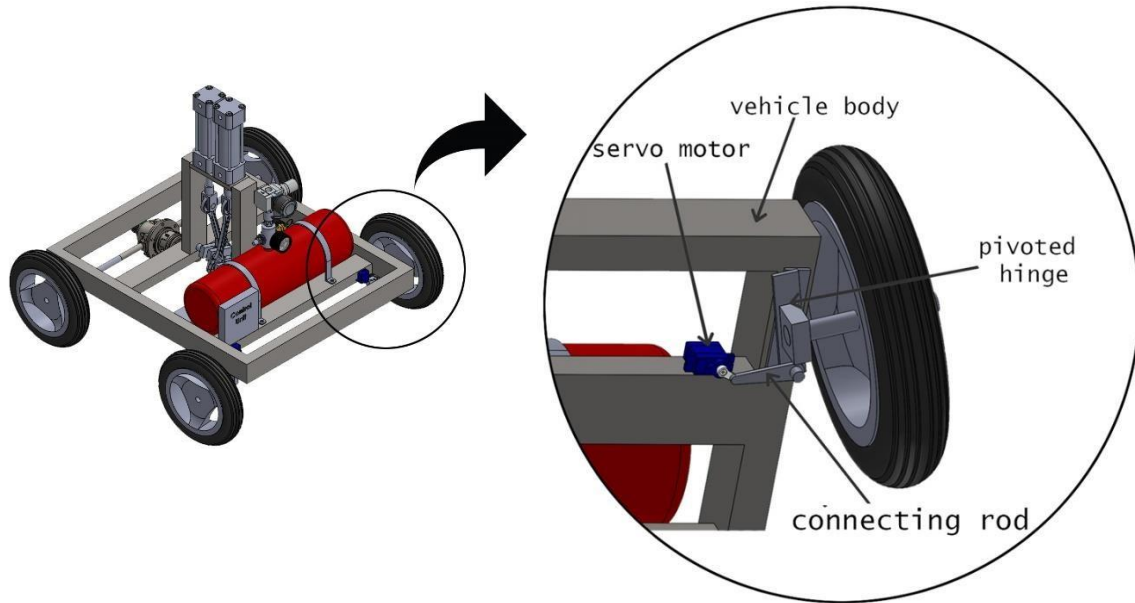
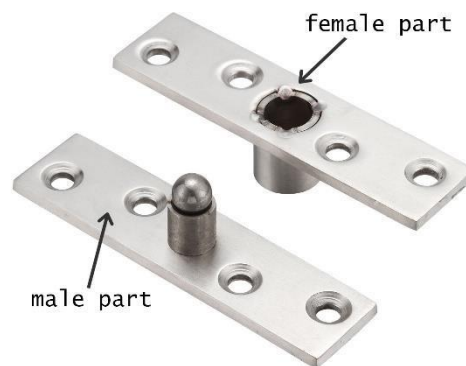


Fig 3.10: the steering mechanism

The pivoted hinge is made of stainless steel and it consists of two portions. The Female part which is mounted on the body of the vehicle. The second part is connected to the wheel shaft via the bearing. The male part is rotated by the operation of the servo motor.

The servo motor is a type of rotary actuators used for precise control of



angular position, velocity and acceleration. It generates high torque so it is capable of carrying up to 12 kg placed at 1 cm on its horn away from the axis of the shaft. Each of the front wheels has its own steering assembly. Both assemblies work simultaneously.

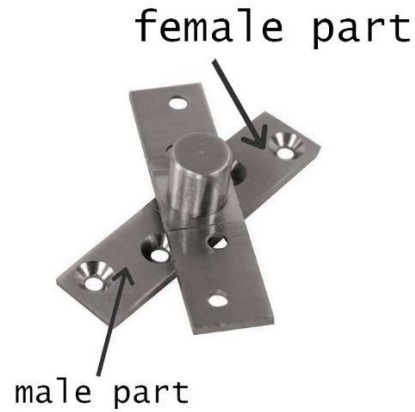


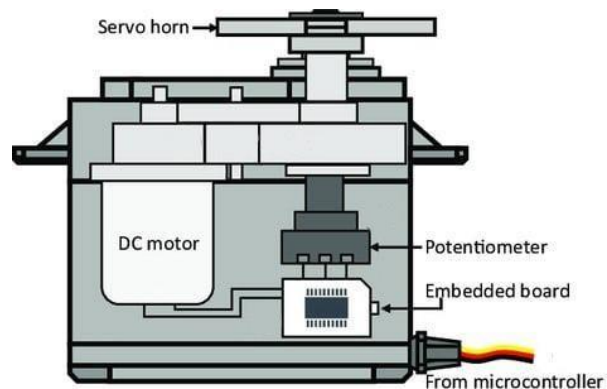
Fig 3.11: pivoted hinge

The horn of the servo motor is normally at 0 degrees when the car is moving forward. To make a right turn, the horn needs to be rotated 90 degrees counter clockwise. Similarly, it should be rotated 90 degrees in the clockwise direction so the vehicle makes a left turn.

For the steering system control, two nrf24l01 wireless modules, two servo motors, Arduino UNO R3, and 9V voltage source for the Arduino UNO R3 and the servomotor. In addition to a one axis joystick to determine the rotation direction. The lever of the joystick is attached to potentiometer. When the lever is displaced from its original position, a voltage difference is produced in the pins. The Arduino UNO R3 is programmed in such a way the servo motors sense this voltage difference then rotate at the same time at the same direction according to the orientation of the lever of the joystick.



Fig 3.12: Servo motor pinout



Fin 3.13: Servo motor construction



Fig 3.14: joystick

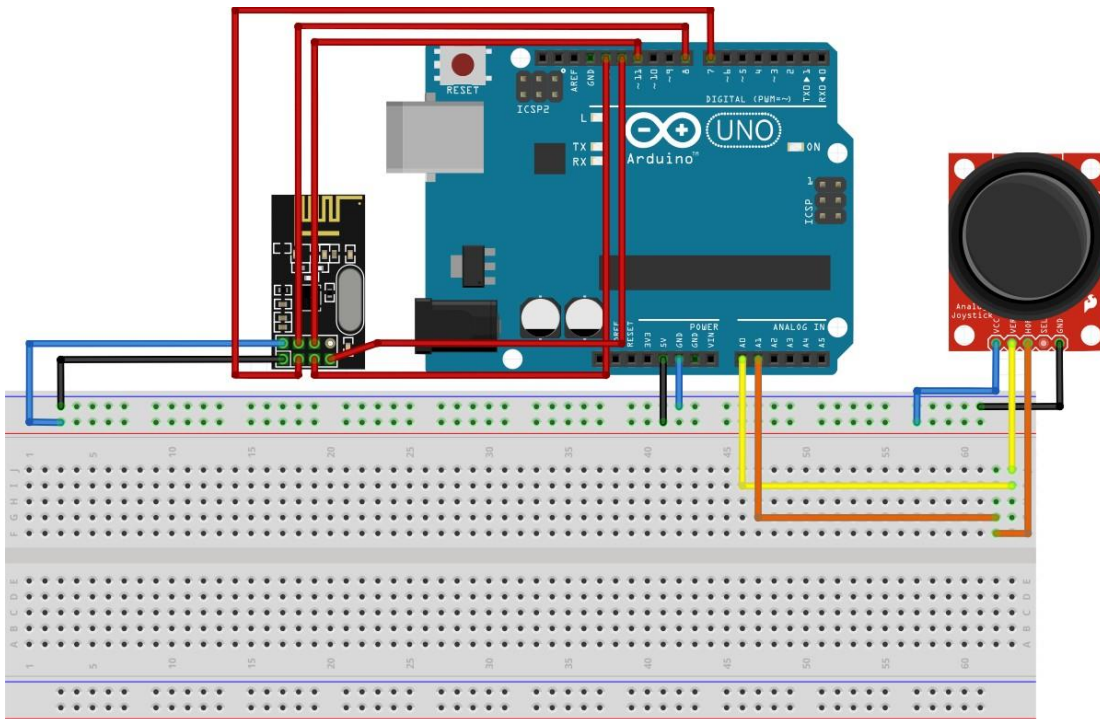


Fig 3.15: The transmitter circuit for the steering system


```
sketch_feb23a §
#include <SPI.h>
#include <nRF24L01.h>
#include <RF24.h>

RF24 radio(7, 8);

const byte rxAddr[6] = "00001";

int sendingdata[6];

void setup()
{
  Serial.begin(9600);
  radio.begin();
  radio.setPALevel(RF24_PA_MAX);
  radio.setAutoAck(false);
  radio.setRetries(15, 15);
  radio.openWritingPipe(rxAddr);

  radio.stopListening();

  delay(50);
}

void loop()
{
  int in1 = analogRead(A0);
  int in2 = analogRead(A1);
  sendingdata[0]=in1;
  sendingdata[1]=in2;

  radio.write( sendingdata, sizeof(sendingdata) );
  Serial.print("RY =");
  Serial.println(sendingdata[0]);
  Serial.print("LY =");
  Serial.println(sendingdata[2]);
  delay(50);
}
```

Fig 3.17: The Arduino code for the transmitting circuit in the steering system

```
sketch_feb23a$
#include <SPI.h>
#include <RF24.h>
#include <Servo.h>

RF24 radio(7, 8);

const byte rxAddr[6] = "00001";
Servo yaw;
Servo thr;
int joystick[6];

void setup()
{
  for(int i = 2; i<=4; i++){
    pinMode(i,OUTPUT); }
  while (!Serial);
  Serial.begin(9600);
  radio.begin();
  radio.setPALevel(RF24_PA_MAX);
  radio.setAutoAck(false);
  radio.openReadingPipe(0, rxAddr);
  radio.startListening();
  thr.attach(2);
  yaw.attach(3);
  delay(50);
}

void loop(){
  if (radio.available())
  {
    bool done = false;
    while (!done)
    {
      // Fetching the data payload
      radio.read( joystick, sizeof(joystick) );
      done = true;

      int val0=map(joystick[0],0,1024,0,180);
      int val1=map(joystick[1],0,1024,0,180);
      thr.write(val0);
      yaw.write(val1);
      Serial.println(val0);
      Serial.println(val1);    } }
    else{
      Serial.println("Data not received");
    }
    delay(50);
  }
}
```

Fig 3.18: The Arduino code for the receiver circuit in the steering system

3.3 The crankshaft design

The crank shaft is a crucial component that turns the piston's reciprocating action into rotary motion via the connecting rod. Crankpin, crankweb, and the shaft at the junction of the crank web make up the crankshaft. The connecting rod connects to the crankpin, which connects to the shaft via the crank web. The shaft spins in the bearings, sending power to the differentials. The crank shaft is seen in Figure 1. The crankshaft should be strong enough to withstand the bending and twisting moments it will experience. Furthermore, it should be rigid enough to keep lateral and angular deflection below acceptable limits..

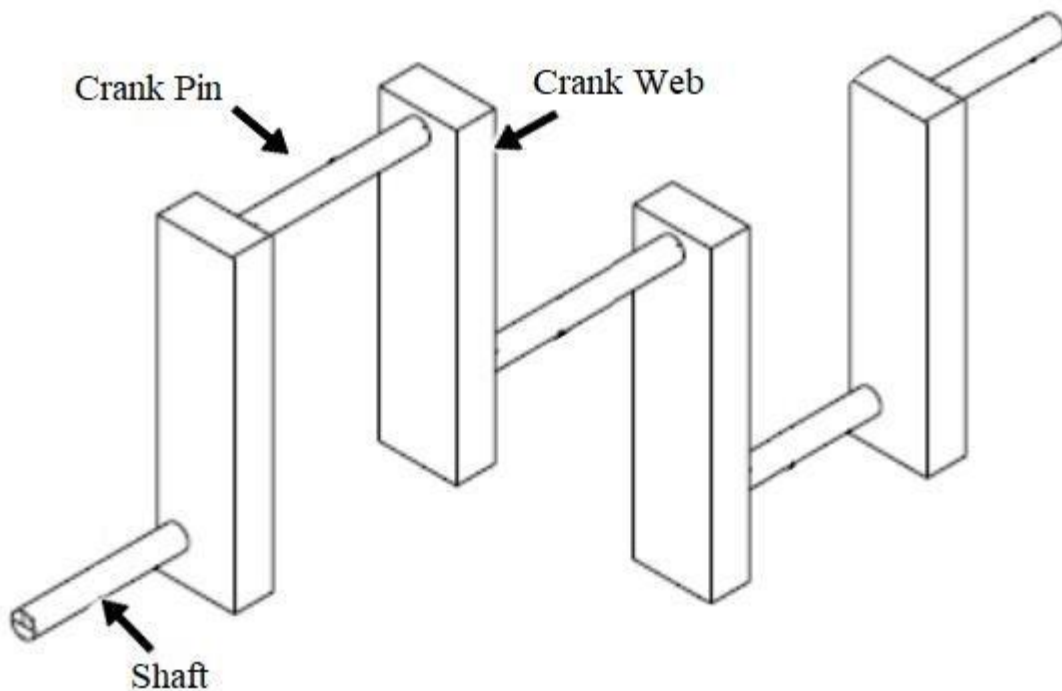


Fig. 1: The crank shaft layout

3.3.1 Crank shaft material

The crank shaft is considered to be manufactured from Cold Drawn AISI 1060 carbon steel with 0.6 wt.% carbon with a tensile strength and a yield strength of 620 MPa and 485 MPa respectively.

3.3.2 Crank shaft analysis and assumptions

To determine the dimensions of the crank shaft different portions, there are two cases of crank position to consider.

Case I: the crank at the top dead center position and subjected to maximum bending moment.

Case II: the crank is at an angle with the line of dead center positions and subjected to maximum torsional moment.

In both cases, the following assumptions are made:

- 1- Crank shaft is assumed to be a simply supported beam.
- 2- The factor of safety is 2 for shear and bending.
- 3- The maximum pressure in the cylinder is 140 psi
- 4- The cylinder bore and stroke are 40 mm and 80 mm.
- 5- The crank radius is 40 mm. ($0.5 \times stroke$)
- 6- The allowable bearing pressure at the crank pin bush is 10 MPa.

3.3.3 Analyzing the crank shaft at top dead center position

Fig. 2 shows the dimensions and the forces acting on the crank

shaft when it is at top dead center position.

b : The distance between bearings a and 2

F_p : Force acting on the crank pin

$(R_1)_v$: The vertical component of the reaction force on bearing 1

$(R_2)_v$: The vertical component of the reaction force on bearing 2

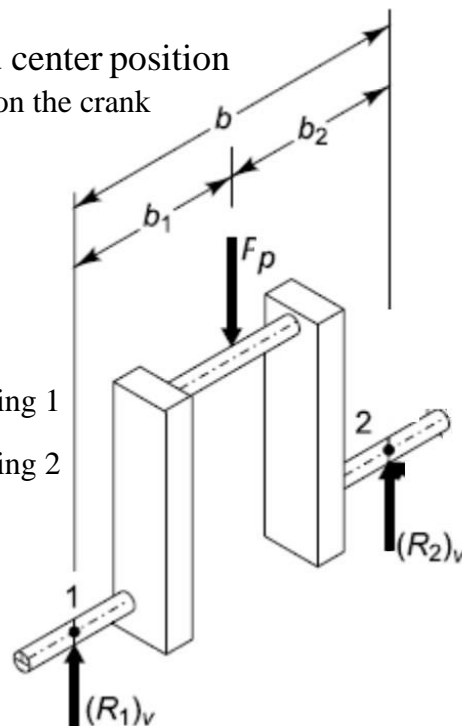


Fig. 2 : the forces acting on the crank shaft when it is in the top dead center

Bearing reactions

According to the manufacturer of the pneumatic actuator;

$$F_p = \text{pressure in pneumatic actuator (bar)} \times 0.126$$

$$F_p = 9.652 \times 0.126 = 1.216 \text{ KN} = 1216$$

$$(R_2) - b_1 F_p = 0 ; \text{ (The resultant moment about bearing 1)}$$

$$(R_2) = \frac{b_1 F_p}{b_2}$$

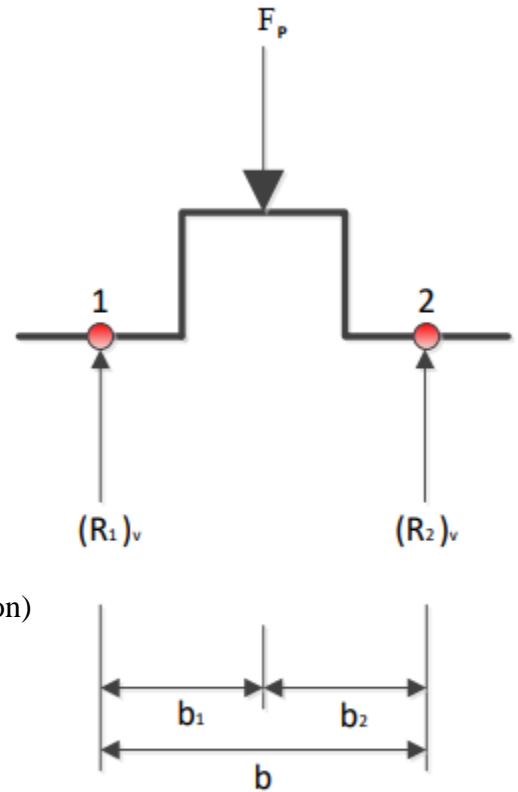
$$b_1 = 45 \text{ m}, b_2 = 45 \text{ mm}$$

$$(R_2) = 0.5 \times F_p = 608 \text{ N}$$

$$(R_1) + (R_2) = F_p ; \text{ (Forces balance in the vertical direction)}$$

$$(R_1) = F_p - (R_2)$$

$$(R_1) = 1216 - 608 = 608 \text{ N}$$



Crank pin design

As shown in Fig. 3,

d_c : The crank pin diameter

l_c : The crank pin length

The bending moment of the crank pin in its center plane is given by;

$$(M_b)_c = (R_1) \times b_1 \dots (1)$$

$$\sigma_b = \frac{(M_b)_c \times y}{I}$$

$$(M_b)_c = \frac{\sigma_b \times I}{y} ; I = \frac{\pi d_c^4}{64} ; y = \frac{d_c}{2} ; \sigma_b = 0.5 \times \sigma_y$$

Where;

I : The second moment of inertia

σ_b : The allowable bending stress for the crank pin material

σ_y : The yield strength for the crank pin material

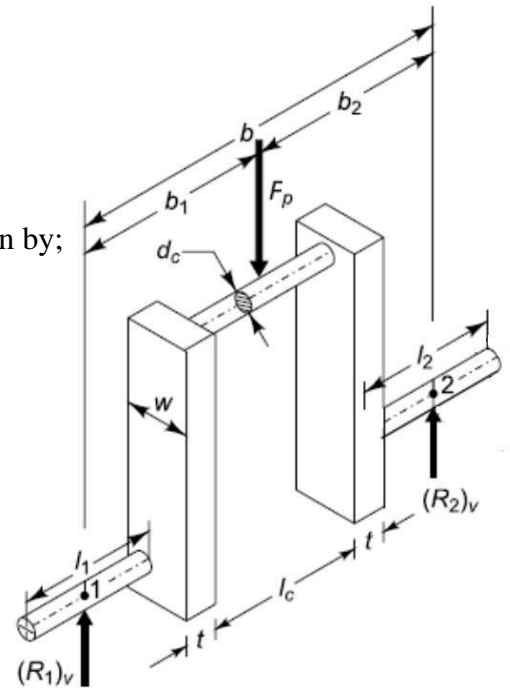


Fig.3 Crank Pin and Web

Substituting;

$$(M_b)_c = \frac{0.5 \times \sigma_y \times \pi \times (d_c^4 / 64)}{c} \dots (2)$$

From equations (1) & (2)

$$d_c = \sqrt[3]{\frac{32 \times (R_1) \times b_1}{0.5 \times \pi \times \sigma_y}}$$

$$d_c = 10.48 \text{ mm}$$

$P_b = \frac{F_p}{l_c \times d_c}$; where P_b is the maximum bearing pressure that can be applied to the crank pin bush

$$l_c = \frac{F_p}{d_c \times P_b} = \frac{1216}{10.48 \times 10} = 11.6 \text{ mm}$$

The crank pin diameter must be at least 10.48 mm while its maximum length is 11.6 mm to withstand the bending moment when the crank shaft in the top dead center position.

d is taken 15 mm and l_c is 10 mm

Crank web design

The minimum values of the dimensions of the crank web are determined using empirical relationships and then verified for stresses.

$$t = 0.7 \times d = 0.7 \times 15 = 10.5 \text{ mm}$$

$$w = 1.14 \times d = 1.14 \times 15 = 17.1 \text{ mm}$$

t = the crank web thickness

w = the crank web width

The crank web thickness and width have to be at least 10.5 mm and 17.1 mm respectively.

t is taken 11 mm and w is 25 mm

As Fig. 3 shows, the central plane of the left-hand crank web is subjected to direct compressive stress and bending stress due to eccentricity of $(R_1)_v$.

$$\text{The direct compressive stress, } \sigma_c = \frac{(R_1)_v}{w \times t} = \frac{608}{25 \times 11} = 2.211 \text{ MPa}$$

$$\sigma_b = \frac{(R_1)_v \times (b_1 - \frac{l_c - t}{2}) \times l}{\frac{w \times t^3}{12}} = \frac{608 \times (45 - \frac{10 - 11}{2}) \times 11}{\frac{25 \times 11^3}{12}} = 41.60 \text{ MPa}$$

The total compressive stress $\sigma_{total} = +\sigma_c = 41.60 + 2.211 = 43.811 \text{ MPa}$

For a safe design, the total compressive stress shouldn't exceed the allowable bending stress for the web material, $\sigma_{allowable}$

$$\sigma_{b,allowable} = 0.5 \times \sigma_y = 242.5 \text{ MPa}$$

The design is secure when the crank shaft is the top dead center position.

The right-hand crank web is made identical to the left-hand web for a balanced crank shaft.

3.3.4 Analyzing the crank shaft when it is subjected to maximum torsional moment

F_p : Force acting on piston due to gas pressure

F_q : Thrust on connecting rod

F_t : Tangential component of force on crank pin

F_r : Radial component of force on crank pin

θ : Angle of inclination of crank with the line of dead centers

ϕ : Angle of inclination of connecting rod with the line of dead centers

L : Connecting rod length

r : Crank radius

Components of force on crank pin

$$\sin \phi = \frac{\sin \theta}{(L/r)} = \frac{\sin 30}{(100/30)}$$

$$\phi = 14.5^\circ$$

$$F_q = \frac{F_p}{\cos \phi} = 1256 \text{ N}$$

$$F_t = F_q \sin(\theta + \phi) = 880.34 \text{ N}$$

$$F_r = F_q \cos(\theta + \phi) = 896 \text{ N}$$

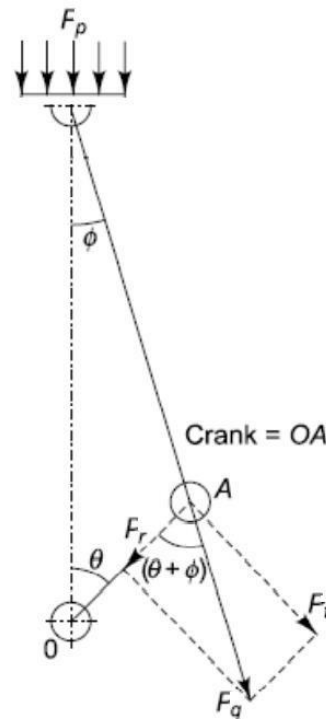


Fig. 4: The crankshaft at angle of maximum torque

Bearing reactions

Due to the tangential component F_t there are reactions $(R_2)_h$ and $(R_1)_h$. Similarly, the reactions $(R_1)_v$ and $(R_2)_v$ are due to the radial component of F_q at the crank pin.

From the moment of horizontal forces about bearing 1;

$$F_t \times b_1 = (R_2)_h \times b ;$$

$$(R_2)_h = \frac{F_t \times b_1}{b} = 440.17 \text{ N}$$

From the moment of horizontal forces about bearing 2;

$$F_t \times b_2 = (R_1)_h \times b$$

$$(R_1)_h = \frac{F_t \times b_2}{b} = 440.17 \text{ N}$$

From the moment of vertical forces about bearing 1;

$$F_r \times b_1 = (R_2)_v \times b$$

$$(R_2)_v = \frac{F_r \times b_1}{b} = 448 \text{ N}$$

From the moment of vertical forces about bearing 2;

$$F_r \times b_2 = (R_1)_v \times b$$

$$(R_1)_v = \frac{F_r \times b_2}{b} = 448 \text{ N}$$

The resultant reaction forces at the bearing are

$$R_1 = \sqrt{[(R_1)_h]^2 + [(R_1)_v]^2} = 628.055 \text{ N}$$

$$R_2 = \sqrt{[(R_2)_h]^2 + [(R_2)_v]^2} = 628.055 \text{ N}$$

Crank pin design

Due to the components of the reaction force at bearing 1, the central plan of the crank pin is associated to bending moment M_b and torsional moment M_t .

$$M_b = (R_1)_v \times b_1$$

$$M_t = (R_1)_h \times r$$

The crank pin diameter (d_c) is calculated by the formula $d_c^3 = \frac{16}{\pi \times \tau} \sqrt{(M_b)^2 + (M_t)^2}$

$\tau = 0.5 \times \text{the tensile strength of the crank pin material}$

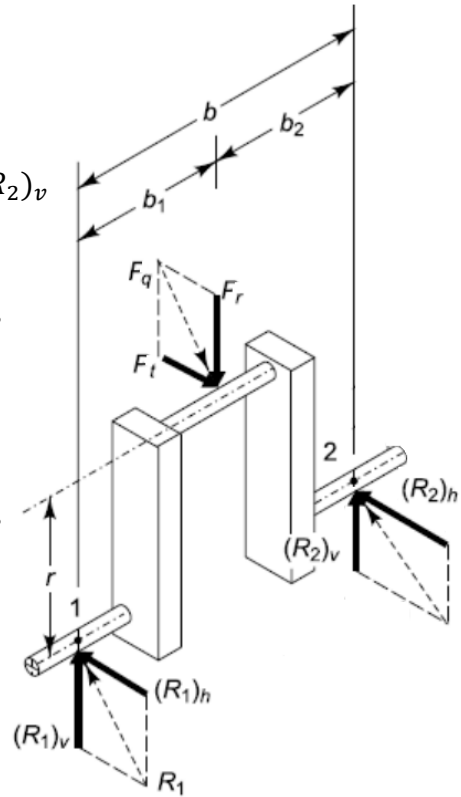


Fig. 5: crank shaft at angle of maximum torque

Where (τ) is the allowable shear stress.

$$\tau = 0.5 \times 620 = 310 \text{ M Pa}$$

$$\begin{aligned} d_c^3 &= \frac{16}{\pi \times \tau} \sqrt{[(R_1)_v \times b_1]^2 + [(R_1)_h \times r]^2} \\ &= \frac{16}{\pi \times 310} \sqrt{[448 \times 45]^2 + [440.17 \times 40]^2} = 440 \end{aligned}$$

$$d_c = 7.6 \text{ mm}$$

The crank pin diameter should be at least 7.6 mm to withstand the maximum torque. The pre-determined crank pin diameter (15 mm) serves a secure design.

$$l_c = \frac{F_q}{d_c \times P_b} = \frac{1256}{7.6 \times 10} = 16.53 \text{ mm}$$

The maximum value of the crank pin length shouldn't exceed 16.53 mm to serve a secure design when the crank pin is subjected to maximum torque. The crankpin length is take as 10 mm to be within the secure span.

Design of shaft at the juncture of right-hand crank web

d_s : the diameter of the shaft at the juncture of right – hand crank web

The shaft is impacted by a torsion moment due to the tangential component of the forces in the vertical and horizontal planes, in addition to the bending moment in both vertical and horizontal directions due to the forces in the vertical and horizontal planes F_q .

$(M_b)_v$: The bending moment in the vertical direction due to $(R_1)_v$ and F_r

$(M_b)_h$: The bending moment in the horizontal direction due to $(R_1)_h$ and F_t

M_t : The torsional moment due to F_t

$$(M_b)_v = (R_1)_v \left[b_1 + \frac{l_c}{2} + \frac{t}{2} \right] - F_r \left[\frac{l_c}{2} + \frac{t}{2} \right] = 15456 \text{ N.mm}$$

$$(M_b)_h = (R_1)_h \left[b_1 + \frac{l_c}{2} + \frac{t}{2} \right] - F_t \left[\frac{l_c}{2} + \frac{t}{2} \right] = 15185.9 \text{ N.mm}$$

$$M_b = \sqrt{[(M_b)_v]^2 + [(M_b)_h]^2} = 21668 \text{ N.mm}$$

$$M_t = F_t \times r = 880.34 \times 40 = 35213.6 \text{ N.mm}$$

$$d_s^3 = \frac{16}{\pi \times \tau} \sqrt{(M_b)^2 + (M_t)^2} = 380$$

$$d_s = 7.25 \text{ mm (The minimum value)}$$

The diameter of the shaft at the juncture of right-hand crank web is considered as 15 mm

Crank web design

A bending stress in both vertical and horizontal planes, direct compressive stress, and torsional stress are all linked with the right-hand crank web.

The bending moment due to radial component;

$$(M_b)_r = (R_2)_v \left[b_2 - \frac{l_c}{2} - \frac{t}{2} \right] \dots (3)$$

$$(M_b)_r = (\sigma_b)_r \times Z; \quad Z = \frac{w \times t^2}{6}$$

$$(M_b)_r = (\sigma_b)_r \times \frac{w \times t^2}{6} \dots (4)$$

Using equations 3 and 4, the bending stress due to radial component $(\sigma_b)_r$ is

$$(\sigma_b)_r = \frac{6 \times (R_2)_v \left[b_2 - \frac{l_c}{2} - \frac{t}{2} \right]}{w \times t^2} = 30.66 \text{ MPa}$$

The tangential component of the bending moment at the junction of the crank web shaft;

$$(M_b)_t = F_t \left[r - \frac{d_s}{2} \right] \dots (5)$$

$$(M_b)_t = (\sigma_b)_t \times Z; \quad Z = \frac{w \times t^2}{6}$$

$$(M_b)_t = (\sigma_b)_t \times \frac{w \times t^2}{6} \dots (6)$$

From equations 5 and 6, the bending stress due to tangential component $(\sigma_b)_t$ is

$$(\sigma_b)_t = \frac{6 \times F_t \left[r - \frac{d_s}{2} \right]}{w \times t^2} = 56.75 \text{ MPa}$$

The direct compressive stress due to radial component is

$$(\sigma_c)_d = \frac{F_r}{2 \times w \times t} = 1.63 \text{ MPa}$$

The total compressive stress σ_c is obtained by

$$\sigma_c = (\sigma_b)_r + (\sigma_b)_t + (\sigma_c)_d = 89.04 \text{ MPa}$$

The torsional moment on the arm is

$$M_t = (R_1)_h \left[b_1 + \frac{l_c}{2} \right] - P_t \left[\frac{l_c}{2} \right] = (R_2)_h \left[b_2 - \frac{l_c}{2} \right] = 17386.715 \text{ N.mm}$$

$$\tau = \frac{M_t}{Z_p} = \frac{4.5 \times M_t}{w \times t^2} = 25.86 \text{ N/mm}^2$$

$$Z_p = \frac{w \times t^2}{4.5} = \text{polar section modulus}$$

The maximum compressive stress is given by

$$(\sigma_c)_{max} = \frac{\sigma_c}{2} + \frac{1}{2}\sqrt{(\sigma_c)^2 + 4 \times \tau^2} = 96 \text{ MPa} < 310 \text{ MPa}$$

Since the maximum compressive stress is less than the allowable compressive stress, the design is safe.

The thickness and width of the left-hand crank web are made identical to that of the right-hand crank web from balancing consideration.

Crankshaft dimensions

1. Crank radius 40 mm
2. Crank pin diameter 15 mm
3. Crank pin length 10 mm
4. Crank web thickness 11 mm
5. Crank web width 25 mm
6. The shaft diameter 15 mm

3.3.5 Testing the crank shaft design using finite element method

To confirm the safety of the crank shaft, the dimensions resulted from the analytical solution were examined using the finite element method in the SolidWorks 2018 software. An obstacle was faced. Which is not finding the AISI 1060 steel in the SolidWorks library. So AISI 1045 steel was used. If the design is safe using the 1045 steel, it is definitely safe using the 1060. Table 1 shows the properties of the material used in this study.

Material Properties	
Name	: AISI 1045 Steel, cold drawn
Model type	: Linear Elastic Isotropic
Default failure criterion	: Max von Mises Stress
Yield strength	: 5.3e+08 N/m ²
Tensile strength	: 6.25e+08 N/m ²
Elastic modulus	: 2.05e+11 N/m ²
Poisson's ratio	: 0.29
Mass density	: 7850 kg/m ³
Shear modulus	: 8e+10 N/m ²
Thermal expansion coefficient	: 1.15e-05 /Kelvin

Table 1: the mechanical properties of AISI 1045.

Firstly, a model of the crank shaft was drawn in the SolidWorks. Then, the geometry is separated to number of small elements is such a process called generating the mesh as shown in figure 6. Next is defining the boundary conditions. In this study, the shaft relying on the bearing is set to be fixed while the force from the piston is applied normally on the crank pin.

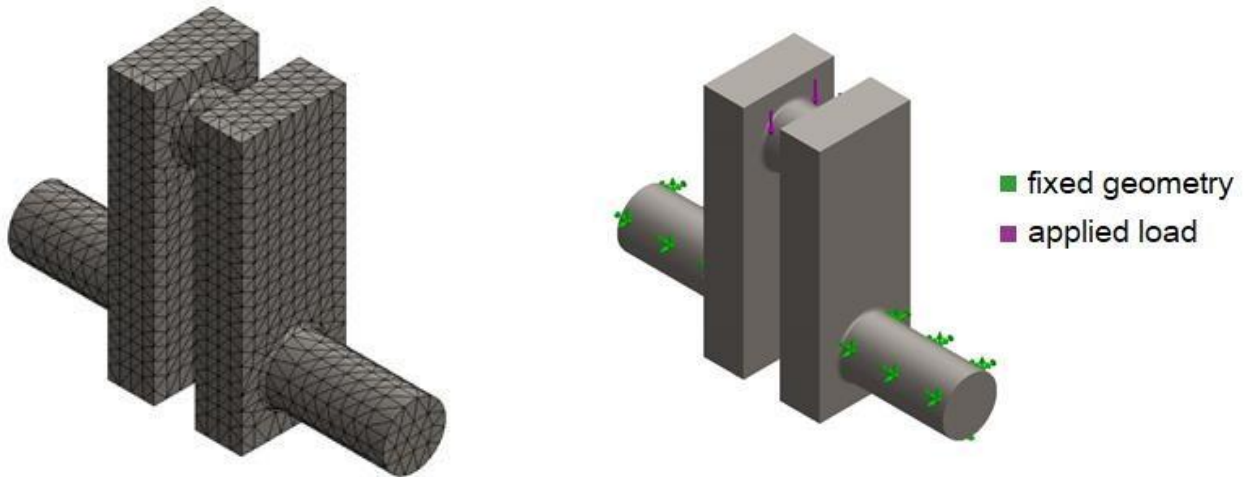


Figure 6: Crank shaft geometry after mesh Figure 7: Boundary conditions of the simulation

Figures 8, 9 and 10 show the result for the stresses on different portions of the crank shaft, the crank shaft deformation and the strain respectively. The maximum stress is ways less than the allowable stress for the material. $1.165e-03$ mm is very small for the deformation. The maximum strain is $6.775e-5$. Since this value is very small the geometry will keep its shape.

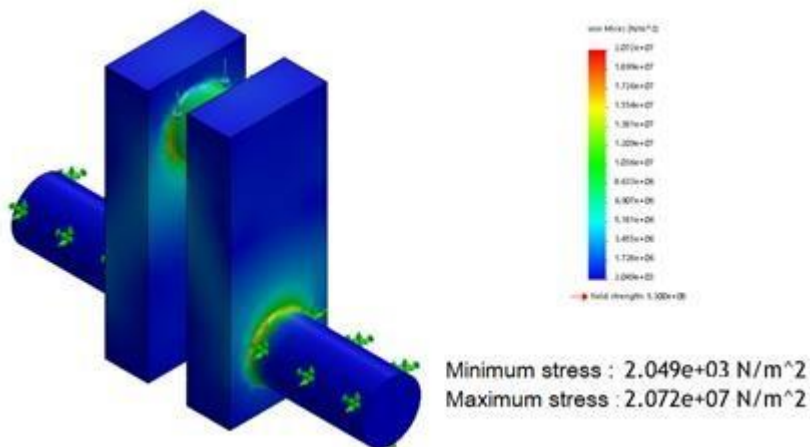


Figure 8: the stresses acting on the crankshaft

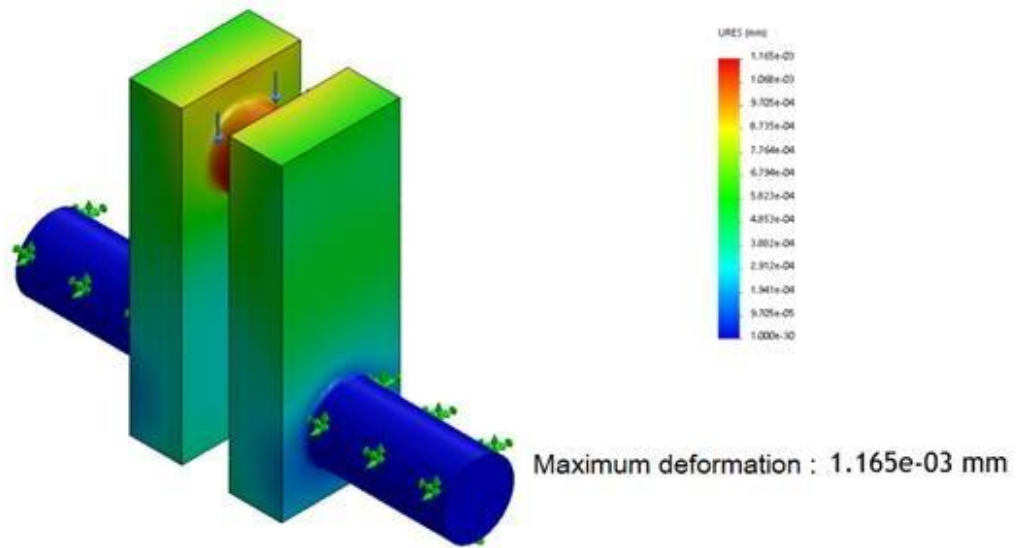


Figure 9: The deformation of the crankshaft

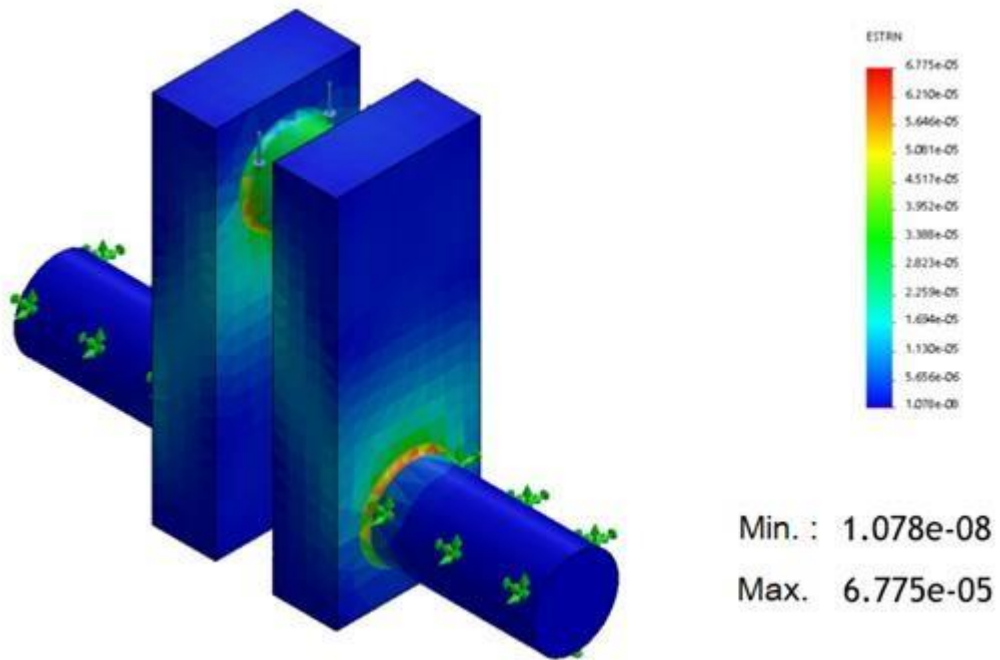


Figure 10: The strain of the crankshaft.

3.4 Connecting rod design

The connecting rod is that part on the engine responsible of transmitting the force from the piston into the crankpin. It is usually made in the shape of I-beam which consists, as shown in figure 1, of two horizontal planes 'flanges' connected with a vertical component 'web'.

The connecting rod, shown in figure 2, has a solid eye from one end in order to connect it with the piston, and a bolted eye from the end connected with the crankpin.

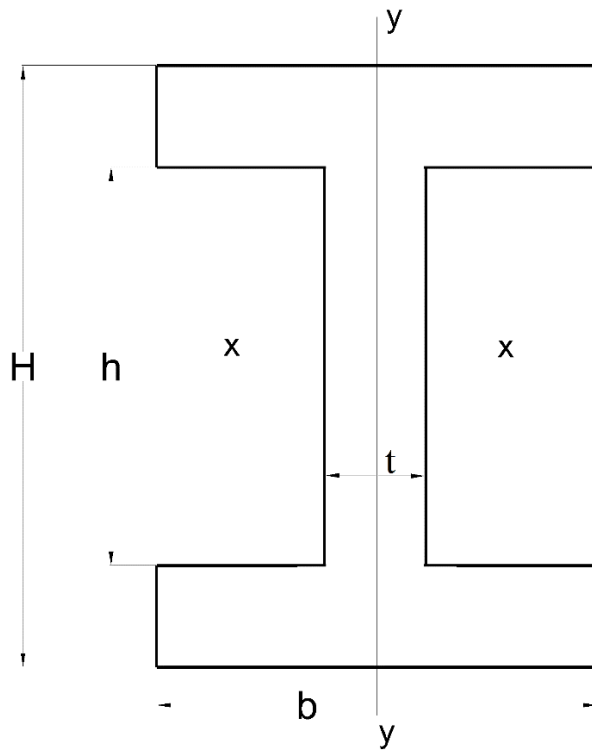


Fig 1: The cross-section of a connecting rod

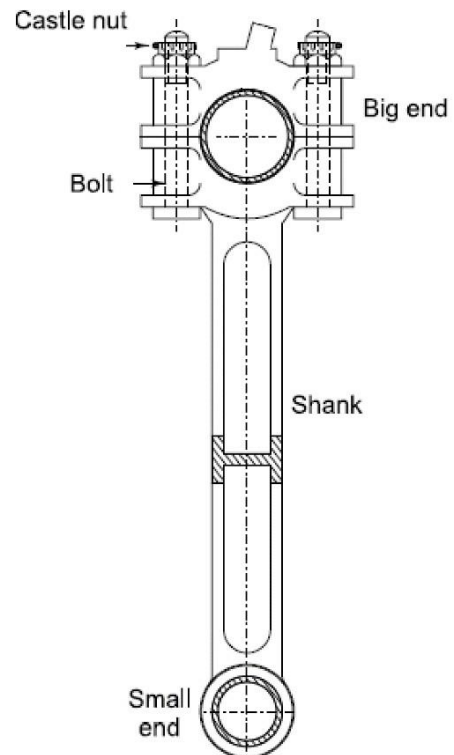


Fig 2: Connecting rod

3.4.1 Connecting rod material

The connecting rods is considered to be made of cold drawn medium carbon steel AISI 1045 steel with a yield strength of 310 MPa, and an ultimate tensile strength of 565 MPa.

3.4.2 Connecting rod dimensions

The connecting rod length

The connecting rods length is usually between 1.4 and 2.2 times the stroke, means it should lie in the range of 112 mm to 176 mm for this prototype. Here, the length of the connecting rod is arbitrary taken as 145 mm.

The shank thickness, height and breadth

The height and breadth of the I-section are functions of its thickness. The thickness is determined to resist the buckling as a result of the force.

It is found that the moment of inertia about the YY-axis needs to be 4 times the moment of inertia about XX-axis since the I-beam tends to buckle about that axis before buckling about the YY-axis. The typical magnitudes of the height and breadth at the middle of the crank shaft that satisfy this statement, as shown in figure 3, are $5t$ and $4t$ respectively. Where t is the thickness. The breadth is constant across the length while the height at the big end can be upto 1.25 times the height at the middle plane.

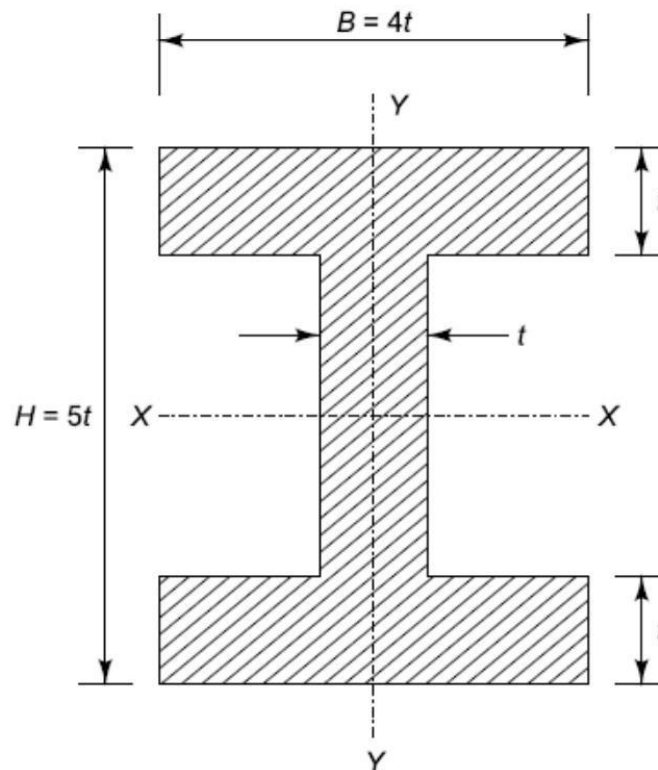


Fig 3: typical dimensions of the connecting rod at the middle

Determining the thickness of the I-beam starts by calculating the critical buckling load considering the factor of safety

$$F_{cr} = n \times F_c$$

F_{cr} ; The critical buckling load

: The force acting on the connecting rod from the piston. n

: The factor of safety ($n = 3$)

$$F_{cr} = 3 \times 1216 = 3648 \text{ N}$$

Then, using Euler's formula in XX-direction.

$$F_{cr} = \frac{K\pi^2 EI_{xx}}{L^2}$$

Where;

K : constant depends on the ends condition. For the connecting rod, both ends are hinged ($K=1$)

L ; Connecting rod length

; Moment of inertia

E ; modulus of elasticity (200 GPa)

Referring to figure 3;

$$I_{xx} = \frac{(4t)(5t)^3}{12} - \frac{(4t-t)(5t-2t)^3}{12} = \frac{419t^4}{12}$$

$$3648 = \frac{\pi^2 \times 200 \times 10^3 \left(\frac{419t^4}{12} \right)}{145^2}$$

By solving this equation, the minimum thickness to withstand the buckling result as 1.027 mm.

So, the dimensions of the connecting rod at the middle are;

The thickness (t) = 2 mm

The breadth (B) = 8 mm

The height (H) = 10 mm, the height at the big end is 12 mm

3.4.3 The ends of the connecting rod

The bearings of the connecting rod

The bearing at the small end of the connecting rod is usually a solid one-piece phosphor bronze bush of 3 mm thickness. The inner diameter of the bush equals the diameter of the piston pin diameter which is 12 mm.

The length of the bush is determined using the l/d ratio. Where l is the length and d is the diameter of the bush.

$$l/d = 2$$

$$l = 2d = 22$$

The big end of the connecting rod is mounted on the crank pin. The bearing here is a lined bush split into two halves with a 0.05 mm bearing crush. The inner diameter of the bush is the diameter of the crank pin which is 15 mm. the length of the bearing can be calculated using the following formula.

$$F_c = d \times l \times P_b$$

Where;

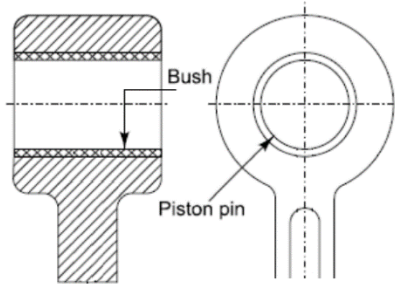
F_c : The force acting on the connecting rod

d : The inner diameter of the bush

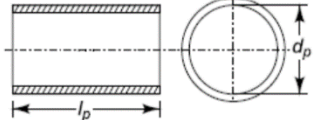
l : The length of the bush

P_b : The allowable bearing pressure

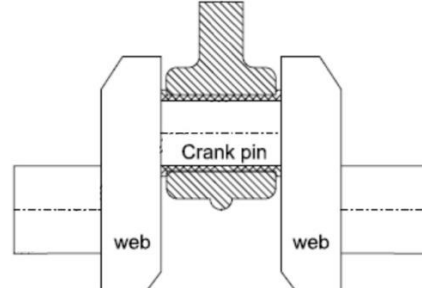
$$l = \frac{F_c}{d \times P_b} = \frac{1216}{15 \times 10} = 8.10, \text{ the bush length is taken as 10 mm.}$$



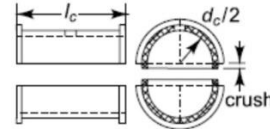
(a) Small end of connecting rod



(b) Bearing bush



(a) Big end of connecting rod



(b) Bearing bush

Fig 4: The small end of the connecting rod Fig 5: The big end of the connecting rod

The bolts and cap of the big end

The bolts of the big end cap are affected only by the inertia force of the reciprocating masses at the top dead center.

The inertia force is given by;

$$F_i = m_r \omega^2 r \left(\cos(\theta) + \frac{\cos(2\theta)}{n_1} \right)$$

F_i : The inertia force

m_r : The mass of the reciprocating parts (arbitrary 2 kg)

ω : The angular velocity of the crank shaft

r : The crank radius

θ : Angle of inclination of crank with the line of dead centers

n_1 : Ratio of length of the connecting rod to the crank radius

At the top dead center, θ is zero.

$$F_i = m_r \omega^2 r \left(1 + \frac{1}{n_1} \right) = 2 \times \left(\frac{2 \times \pi \times 60}{60} \right)^2 \times 40 \times \left(1 + \frac{40}{145} \right) = 4025.5 \text{ N}$$

The two bolts are subjected by equally distributed tensile force. Therefore, the inertia force affects the bolts is

$$F_i = 2 \left(\frac{\pi d_{core}^2}{4} \right) \sigma_c$$

d_{core} : The core diameter of the bolts

σ_c : The permissible tensile stress for bolts material

The bolts are made of alloy steel with an ultimate tensile strength of 720 MPa

$$\sigma_c = \frac{\text{ultimate tensile strength}}{\text{factor of safety}} = \frac{720}{2} = 360 \text{ MPa}$$

$$d_{core} = \sqrt{\frac{4F_i}{2\pi\sigma_c}} = \sqrt{\frac{4 \times 4025.5}{2 \times 3.14 \times 360}} = 2.67 \text{ mm}$$

$$\text{The nominal diameter of the bolts } d_{nominal} = \frac{d_{core}}{0.8} = 3.3375 \text{ mm}$$

Hence, M5X0.8 bolt is used.

The cap is also subjected to the inertia force. The cap is considered as a beam freely supported at the bolts centers and loaded is such a way that the bending moment is $\frac{wl}{6}$

$$M_b = \frac{P_i l}{6}$$

M_b : The bending moment

l : The distance between bolts centers

$l = \text{crankpin dia} + 2 \times \text{bush thickness} + \text{nominal diameter of bolts} + 6 \text{ mm clearance}$

$$l = 15 + 2 \times 3 + 5 + 6 = 32 \text{ mm}$$

$$M_b = \frac{4025.5 \times 32}{6} = 21469.33 \text{ N.mm}$$

$$M_b = \frac{I \sigma_b}{y}$$

$$I = \frac{b_c t_c^3}{12} ; y = \frac{t_c}{2}$$

$$t_c = \sqrt{\frac{6 \times M_b}{b_c \times \sigma_b}}$$

$$\sigma_b = 0.5 \times \sigma_y = 125 \text{ MPa}$$

b_c : The cap width; equals crank pin length

t_c : The cap thickness

σ_b : Permissible bending stress for the cap

σ_y : The yield strength for the cap

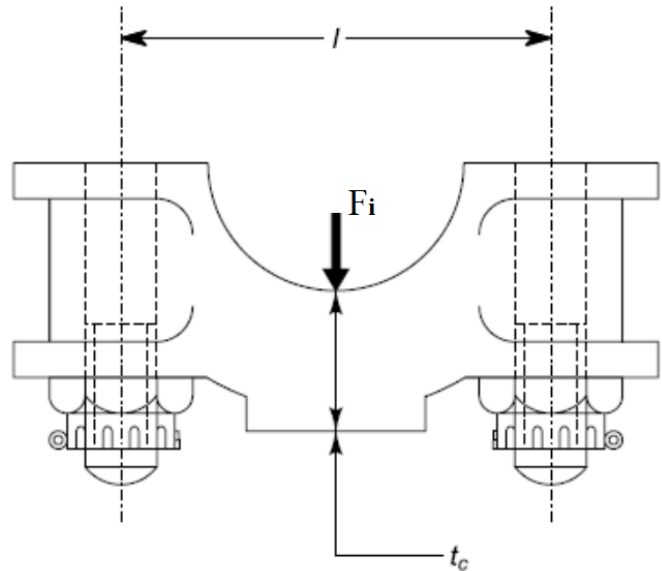


Fig 6: The force acting on the cap

$$t_c = \frac{\sqrt{6 \times M_b}}{b_c \times \sigma_b} = \sqrt{\frac{6 \times 21469.33}{15 \times 125}} = 8.3 \text{ mm}$$

The width of the cap is 10 mm.

Connecting rod dimensions:

- | | |
|---|--------|
| 1. Connecting rod length | 145 mm |
| 2. Thickness of the cross-section | 2 mm |
| 3. Connecting rod breadth | 8 mm |
| 4. Connecting rod height at the small end | 10 mm |
| 5. Connecting rod height at the big end | 12 mm |
| 6. Small eye diameter | 12 mm |
| 7. Big eye diameter | 15 mm |
| 8. Cap thickness | 10mm |

3.4.4 Testing the connecting rod design using finite element method

The dimensions from the analytical solution are tested using the finite element method in the SolidWorks 2018 software to insure the safety of the connecting rod against buckling. Table 1 shows the properties of the material used in this study.

Material Properties	
Name	: AISI 1045 Steel, cold drawn
Model type	: Linear Elastic Isotropic
Default failure criterion	: Max von Mises Stress
Yield strength	: 5.3e+08 N/m ²
Tensile strength	: 6.25e+08 N/m ²
Elastic modulus	: 2.05e+11 N/m ²
Poisson's ratio	: 0.29
Mass density	: 7850 kg/m ³
Shear modulus	: 8e+10 N/m ²
Thermal expansion coefficient	: 1.15e-05 /Kelvin

Table1: the mechanical properties of AISI 1045.

First step in the numerical solution is to create a model of the connecting rod then generating the mesh. A model of the connecting rod was drawn SolidWorks 2018. Figure 7 and 8 show the model before and after the mesh was generated. The boundary conditions are then defined. In our study, the face of the big end in contact with the crank pin is set to be fixed while the force is applied on the surface of the small end in contact with the piston pin.

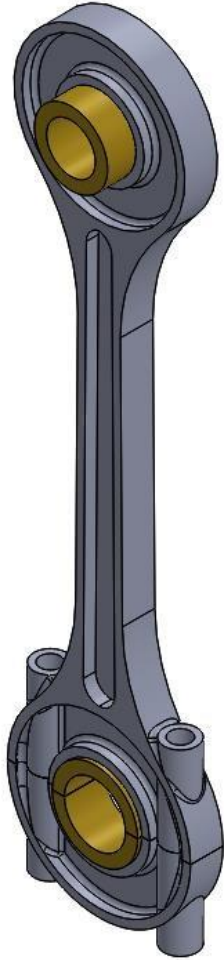


Figure 7: A model of the connecting rod



Figure 8: The model after mesh is generated

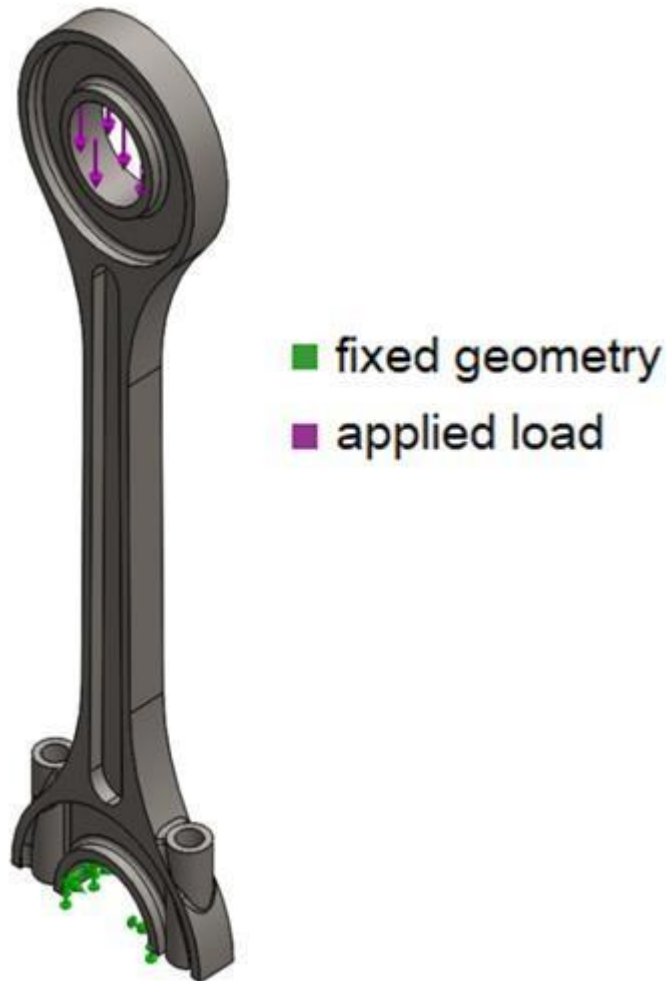


Figure 9: the boundary condition defined on the connecting rod

Figures 10, 11 and 12 show the result for the stresses on different portions of the connecting rod, the connecting rod deformation and the strain respectively. The maximum stress is less than the allowable stress for the material. The maximum, deformation is $5.442e-02$ mm which is very small. The connecting rod will keep its shape since the maximum strain is a very small, $4.523e-04$.

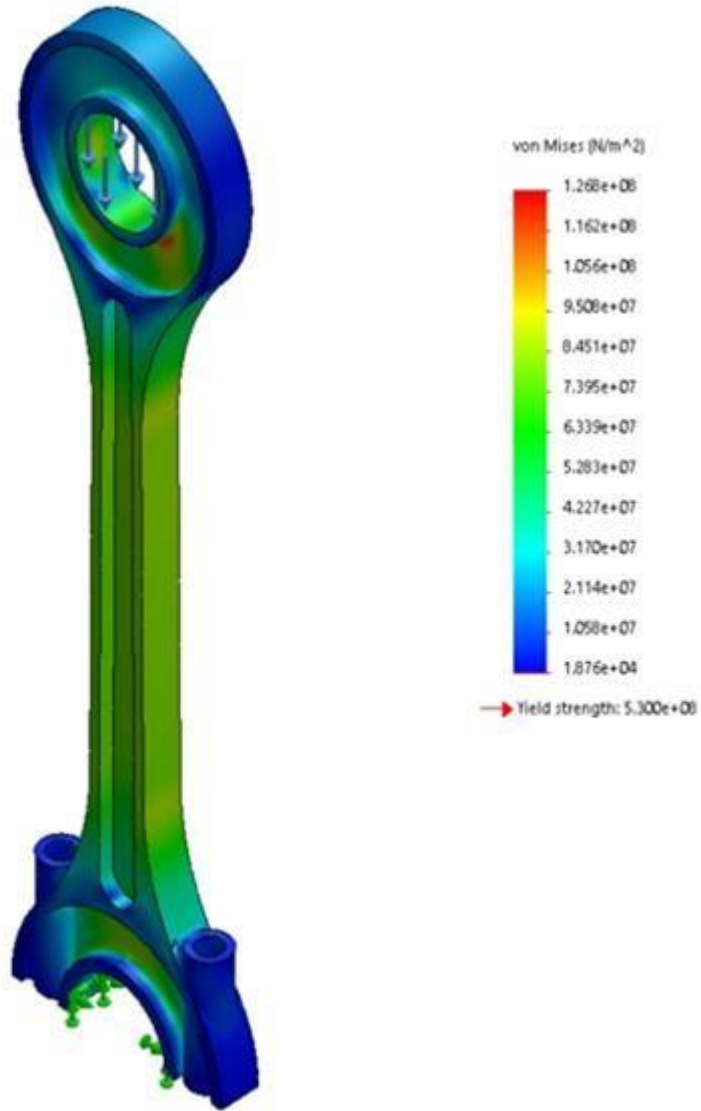


Fig 10: stresses on the connecting rod

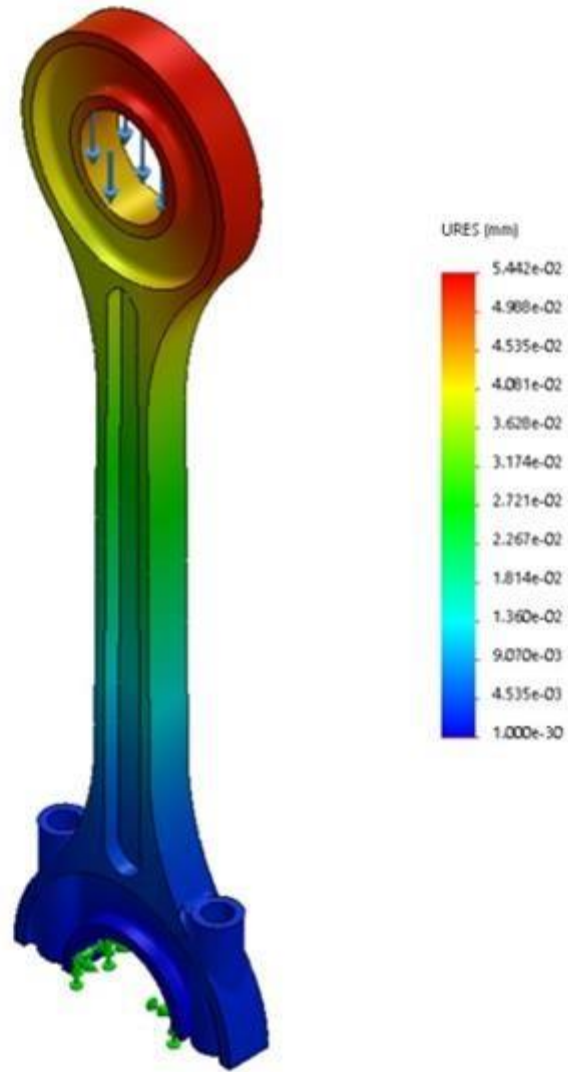


Fig 11: deformation of the connecting rod

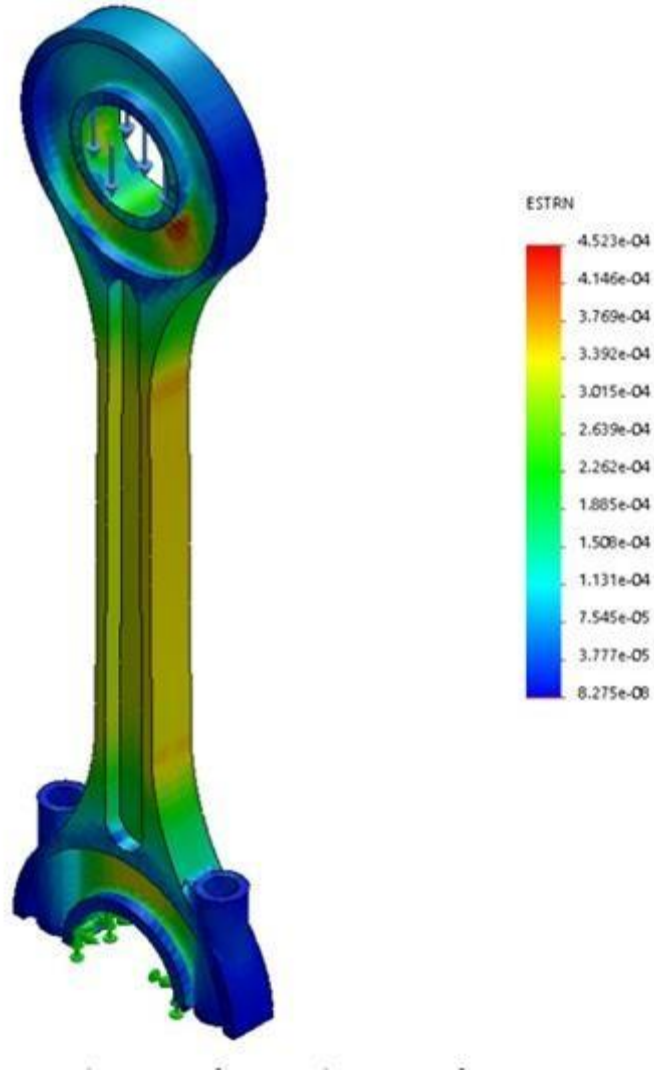


Fig 12: strain of the connecting rod

3.5 Chassis design

The chassis is the metal parts that connects allow components and systems of the vehicle together. It is made of mild steel AISI 1015(3.07 kg/m). 50x25x3 mm rectangular tube cross section was used to reduce the weight of the vehicle.

The dimension of the cross section of the chassis were chosen arbitrary and tested for stresses. Considering the dimensions of all components and allowances, the chassis measures 450 mm in width and 600 mm in length.

The pneumatic actuators are bolted on mild steel rectangular bar.

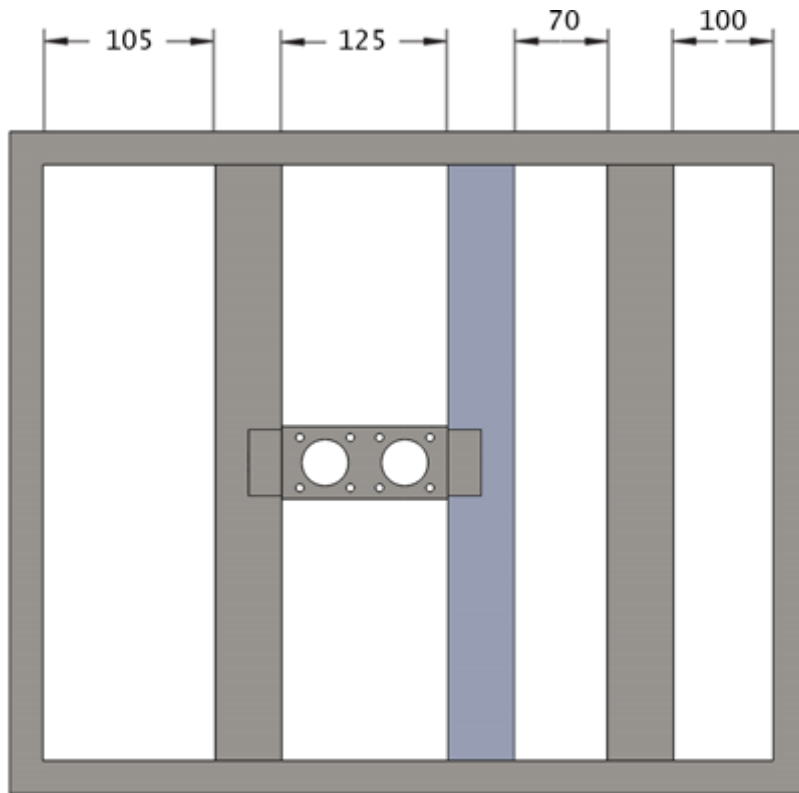


Fig: Top view of the chassis

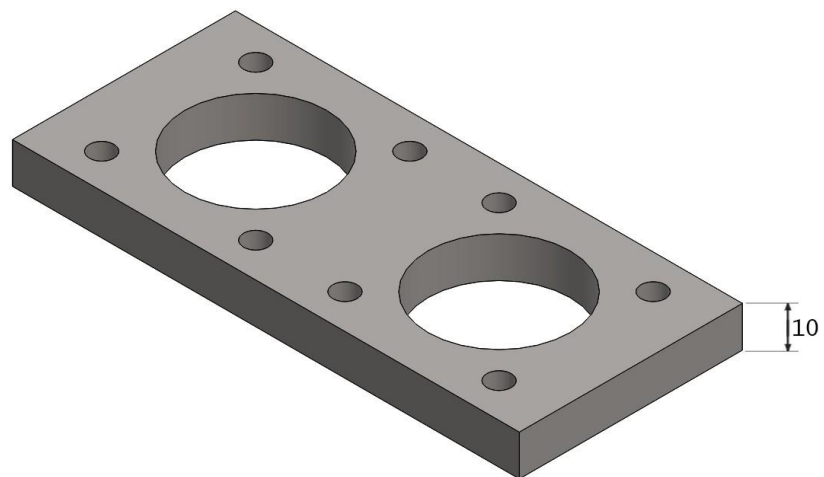


Fig: Isometric view of the bar holding the pneumatic actuators

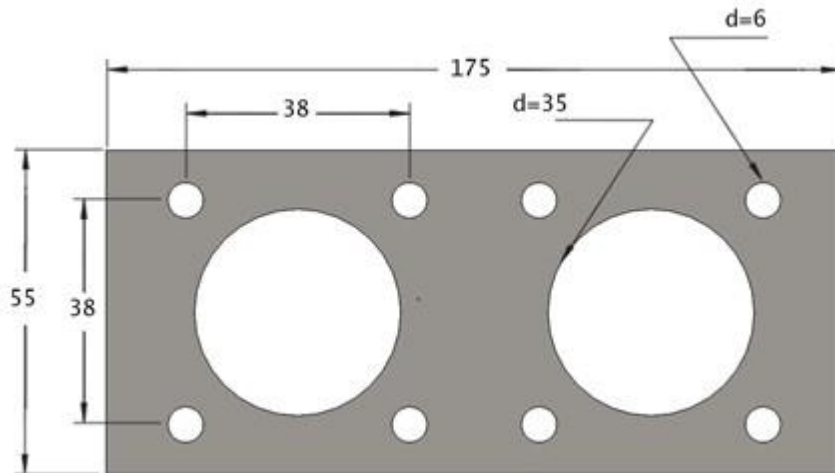


Fig: Top view of the bar holing the pneumatic actuators

To confirm the safety of the chassis design, the beam carrying the maximum load was analyzed using finite element method in SolidWorks 2018.

The maximum load is applied on the beam beneath the air tank due to the mass of the air in the tank. The analysis also includes the weight of the beam.

The table below shows the properties of the steel used for manufacturing the chassis.

Material Properties	
Name:	AISI 1015 Steel, Cold Drawn (SS)
Model type:	Linear Elastic Isotropic
Default failure criterion:	Max von Mises Stress
Yield strength:	3.25e+08 N/m ²
Tensile strength:	3.85e+08 N/m ²
Elastic modulus:	2.05e+11 N/m ²
Poisson's ratio:	0.29
Mass density:	7870 kg/m ³
Shear modulus:	8e+10 N/m ²
Thermal expansion coefficient:	1.2e-05 /Kelvin

Table: properties of the chassis material

Model name: Part1
Support: Fixed Support (Default)
Mesh Type: Solid Mesh

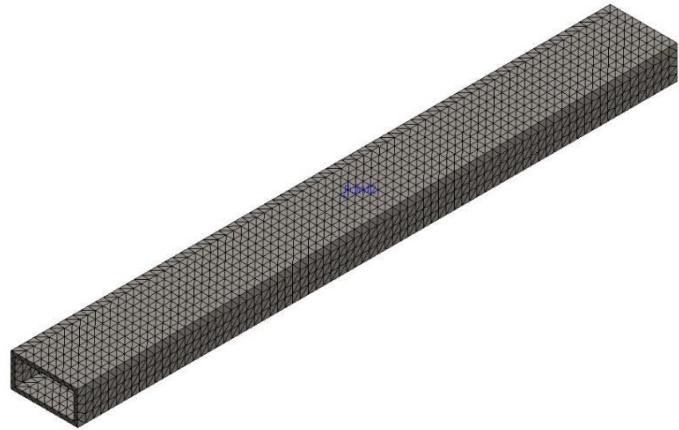


Fig: a model of the beam carrying the maximum load after mesh generation

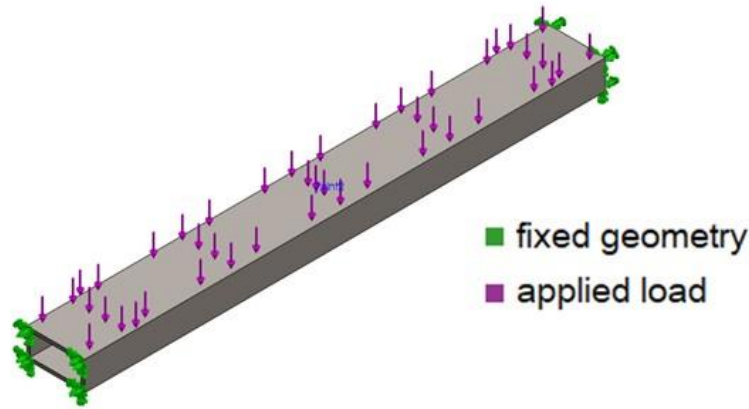


Fig: The boundary conditions applied to the beam carrying the maximum load

The results of this analysis are shown in the following figures. As we can see, the stresses, deformation and the strain values represent a secure design.

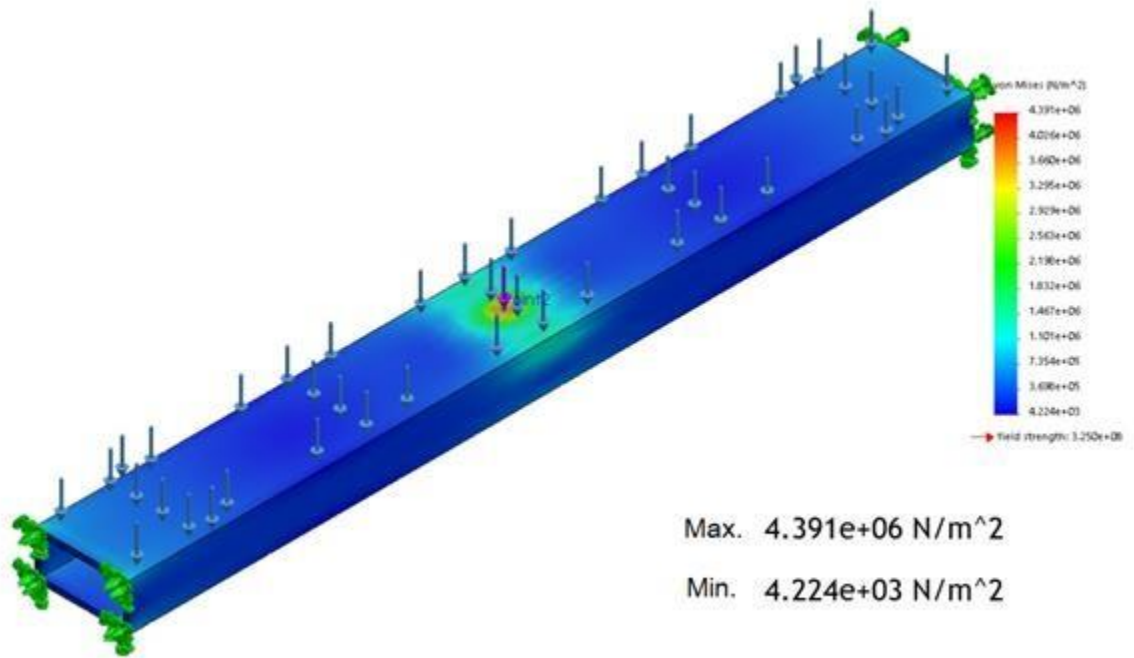


Fig: The stresses on the beam carrying the maximum load

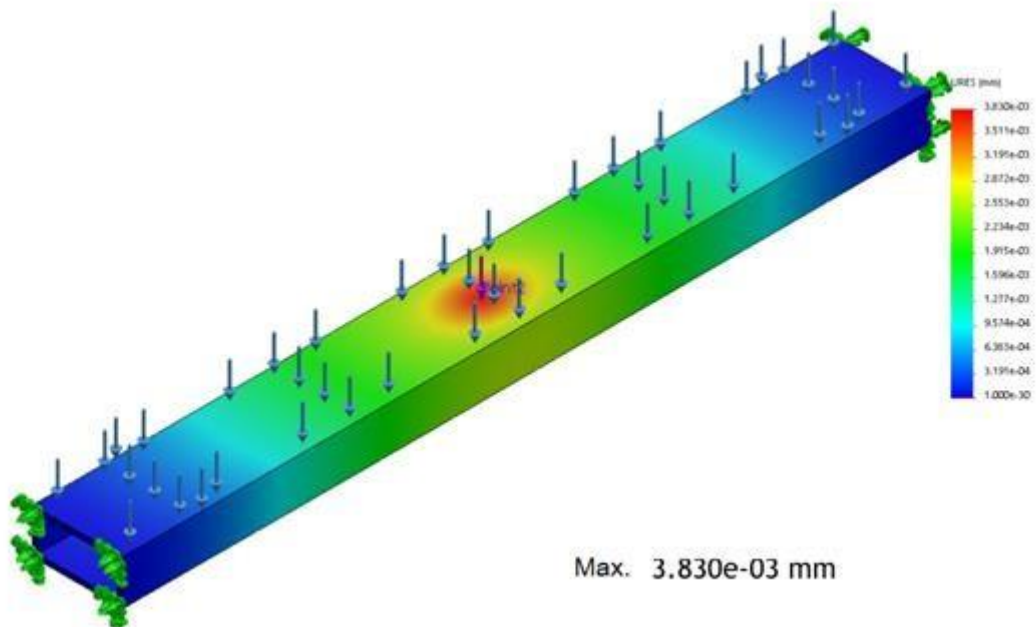


Fig: The deformation of the beam carrying the maximum load

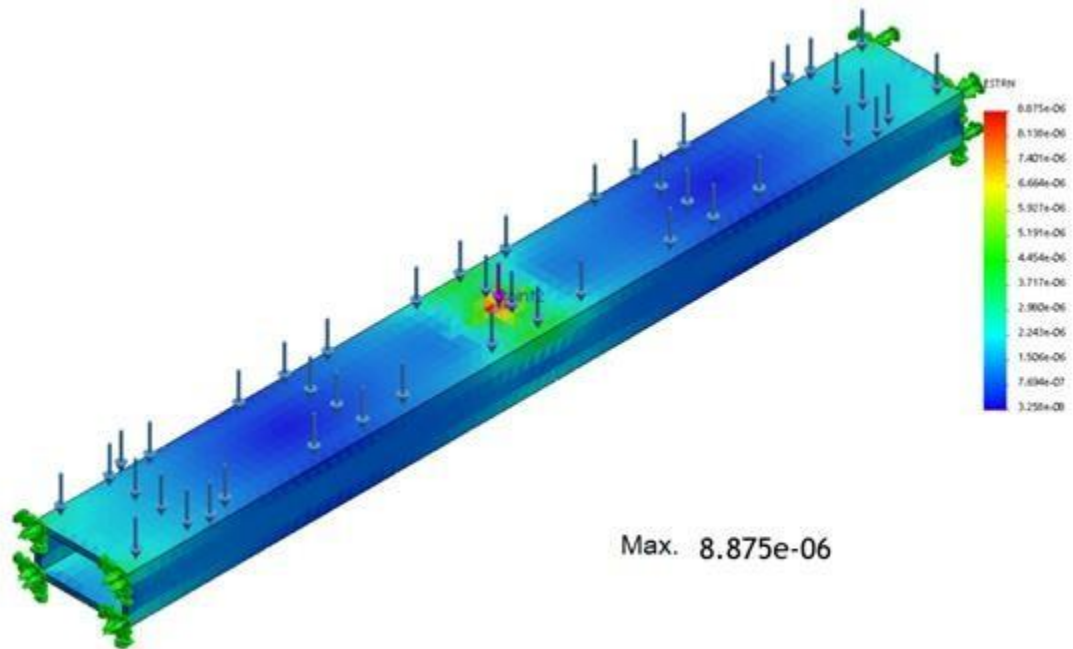
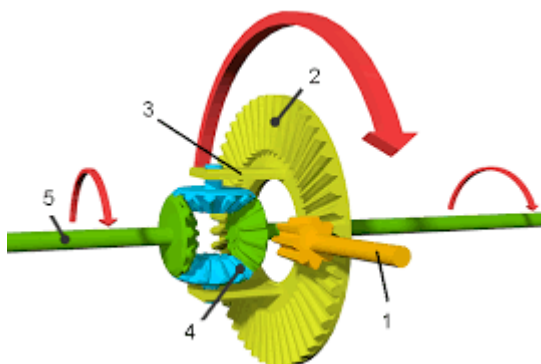


Fig: The strain of the beam carrying the maximum load

3.6 Differentials

Differentials is a system that transmits an engine's torque to the wheels. The differential takes the power from the engine and splits it, allowing the wheels to spin at different speeds. Each wheel is able to turn independently from the other such as when the car is turning. The differentials assembly consists of a pinion gear attached to the propeller shaft, bevel gear, connecting edge, and side gear in addition to left and right axle shafts.



- 1: pinion gear and the propeller shaft
- 2: bevel gear.
- 3: connecting edge.
- 4: side gear.
- 5: left axle shaft
- 6: right axle shaft

differentials assembly

Input parameters

$$\text{Gear ratio} = \frac{t_{out}}{t_{in}} = \frac{N_{in}}{N_{out}} = \frac{T_{out}}{T_{in}} \quad (t = \text{No. of teeth: } N = \text{rotational speed: } T = \text{torque}) = 32/8 = 4$$

$$\text{Input power} = \frac{2 \cdot 3.14 \cdot N_A \cdot T_A}{60} = 62.8 \text{ W (PI)}$$

$$\text{Output power} = m (\text{efficiency}) \cdot P_{in} = .85 \cdot 62.8 = 53.38 \text{ W (PO)}$$

Input torque 10 NM (Ti) expected value

$$\text{Output torque} = T_B = \frac{60 \cdot P_{out}}{2 \cdot 3.14 \cdot N_B} = 33.9827 \text{ W so the } T_B \text{ ideal} = 33.98 = \text{so the (the torque actual)} = \text{ideal torque} \cdot m = 33.98 \cdot .85 = 28.883 \text{ that's the actual value}$$

Input speed 60rpm (NA) same as the shaft rotation speed

$$\text{Output speed: GR} = \frac{N_{in}}{N_{out}} \text{ so } N_o = 60/4 = 15\text{rpm}$$

$$\text{Module} = \text{pitch diameter} / \text{number of teeth} = 1$$

The material used on the pinion and gear is medium carbon steel whose allowable bending stress maybe taken as 230 MPA where modulus elasticity taken as 210GPA

Design of inner bevel

Pitch geometry (D) 15 mm

Pitch cone angle (Y) 45

Back cone angle (B) 45

Pressure angle 20

Module 2 mm

Inner bevel set

Pitch cone distance (AO)

$$= \sqrt{\left(\frac{D_1}{2}\right)^2 + \left(\frac{D_2}{2}\right)^2} = \text{where } D_1 = D_2 = 20 \quad AO = 6.32 \text{ mm}$$

Face width (b)

$$B = \frac{AO}{3} = 6.324/3 = 2.108 \text{ mm}$$

Height addendum

$$H_a = 1 \cdot m = 1 \cdot 2 = 2 \text{ mm}$$

Height of Dedendum (hf)

$$H_f = 1.25 \cdot m = 1.25 \cdot 2 = 2.5$$

Mean radius (R mean) = $(D/2) - (b/2)\sin Y = (20/2) - (3.726/2)\sin 45 = 8.42\text{mm}$

Minimum number of teeth (zmin) = $\frac{2 \cdot 2 \cos(45)}{(\cos 20)^2} = 4.9$ near to 5 = 5 teeth

So the actual number of teeth $D = m \cdot Z = 10/2 = 5$

Since the Z actual = Z min so it's permissible

Force analysis of inner bevel set

Tangential force (FT) = $T/R_{\text{mean}} = 28.875/15 = 1.925 \text{ NM}$

Radial force on pinion $F_R = F_T \cdot \tan(Y) \cdot \cos(45) = 2.2629 \text{ N}$

Pitch line velocity

$V_m = \frac{3.14 \cdot D \cdot \omega}{60000}$ (where D is the mean diameter = $2 \cdot R_{\text{mean}}$) = 0.0132 m/s

Equivalent teeth on pinion

$Z_{ep} = Z_p / \cos(45) \cdot \text{soc}(45) \text{ power } 3 = 5 / \cos 45 \cdot \cos 45 \text{ power } 3 = 66 \text{ teeth}$

So we have to find the Lewis factor (Y) = $.921 / Z_{ep} = .154$ ($.921/66$) = .141

So the material selection is alloy steel-15Ni4Cr1

Sut (ultimate strength stress in shear) = 1500 NMM^2

BHN = 650

Safety factor shall be considered as 1.5

$\sigma_a = \text{allowable bending stress}$

= $S_{ut}/3 = 1500/3 = 500 \text{ N/MM}$

Stress based analysis of inner bevel set

$S_b = \sigma_a \cdot C_v \cdot b \cdot 3.14 \cdot m \cdot Y \cdot \frac{A_{o,b}}{A_o}$
 = $500 \cdot .7462 \cdot 2.108 \cdot 3.14 \cdot 2 \cdot .141 \cdot .665 = 463.122 \text{ N}$

The ratio factor is 1 meter gears

Shear stress on hollow bevel drive shaft

Inner diameter (di) = 15mm

Outer diameter (do) = 23mm

The permissible shear stress = $\frac{.5}{FOS} = 500 \text{ N/MM}^2$

The actual shear stress = $\frac{16T}{3.14 \cdot D^3 \cdot (1_c^4)} = 33.95$

Since the actual shear is less than the permissible one so design is permissible

Sun gear parameters

Module=2

Teeth=32

Pressure angle=20

Face width=2.108mm

Hub diameter=18mm

Mounting distance=32mm

Nominal shaft diameter=13mm

Pinion gear

Teeth=8

Pressure angle=20

Face width=2.108

Hub diameter=12

Nominal shaft diameter=10mm

Mounting distance=32

Crown gear

Module=2

Teeth 32

Pressure angle=20

Face width=2.108mm

Hub diameter=40mm

Nominal diameter=20mm

Mounting distance=25mm

Driving gear

M=2

Teeth=8

Pressure angle=45

Face width=2.108mm

Hub diameter=20mm

Mounting distance=50mm

Nominal shaft diameter=15mm

3.7 bearings design

Bearings are made of hard steel that guide and support shafts and axles. They are part of the chassis, guide the wheels and absorb axial and radial forces. Radial forces are longitudinal forces produced as a result of rotation. They are applied to the bearing at a right angle to the longitudinal axis.

Essentially, ball bearings consist of

- Outer and inner rings
- The rolling elements
- A ball cage enclosing the rolling elements.

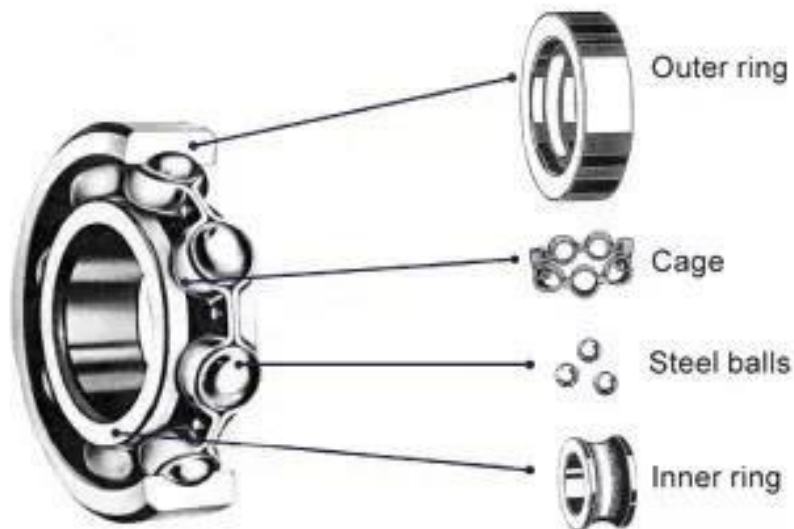
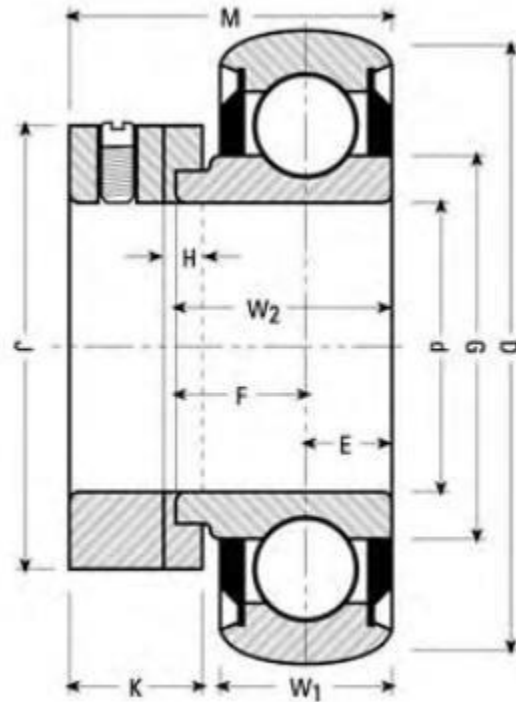


Fig: construction of ball bearings

Commercial 306s roller bearings were used for the wheels and the crank shaft. The following figures shows the dimensions of the used bearings.



"NPS" Series

Spherical O.D.	Basic Outer Ring	Bore d		O.D. D		Inner W2		Outer W1		E	F	G	H	J	K	M	R	Collar
		Inch	mm	Inch	mm	mm	mm	Inch	Inch									
NPS-008-RRC	203	1/2	40	1.575	0.750	13	0.512	0.256	0.494	0.957	0.156	1.125	0.531	1.125	0.126	C008		
NPS-010-RRC	203	5/8	40	1.575	0.750	13	0.512	0.256	0.494	0.957	0.156	1.125	0.531	1.125	0.126	C010		

Fig: Dimensions of the ball bearing

These bearing are from Motions Industries. The model NPS-008-RRC is used to reduce the friction between the wheels shaft and the chassis. While NPS-010-RRC is used for the crankshaft.

CHAPTER FOUR RECENT ADVANCEMENTS

4.1 Technology Air storage refueling

Using an absorption material within the tank, compressed air might be stored at a lower pressure. Compressed natural gas is stored at 500 psi rather than 4500 psi using absorption materials like activated carbon or a metal-organic framework, which saves a lot of energy. One company stores air in tanks that carry about 3,200 cubic feet (roughly 90 cubic meters) of air at 4,500 pounds per square inch (around 30 MPa). The tanks may be filled quickly at home or in parking lots by connecting the car to the electrical grid through an onboard compressor, or in a few hours at a service station equipped with heat exchangers. The Tata/MDI air car's tanks were rated at 4,350 psi, necessitating the installation of new high-tech air pumps at stations, which would represent a significant financial expenditure for the station's owner.

4.2 Input Energy

Producing compressed air at high pressures is exceedingly expensive, and using it is inefficient. A typical consumer vehicle of traditional size and shape consumes 0.3-0.5 kWh (1.1-1.8 MJ) per mile of use at the drive shaft, however, unconventional sizes may consume much less. It's vital to remember that the electrical grid provides the energy required to compress the air into the tanks. The utilization of fossil fuels is commonly used to support such electric systems. However, initiatives are underway to compress air using non-conventional energy sources such as solar and wind. The energy density of compressed air is low.

4.3 Temperature Control

The adiabatic process of air compression maintains the heat of compression. That is, no change in heat transfer or entropy occurs, and compressed air becomes extremely hot. The compressed air temperature rises as a result of the energy delivered from the compressor to the gas. An isothermal or adiabatic compression procedure can be used to control this. The temperature of the gas in the system remains constant during the isothermal compression operation. This necessitates the removal of heat from the gas. Between the compressor stages, heat can be extracted using a heat exchanger (intermediate cooling). The inter cooler should be constructed to achieve high heat exchange rates and low pressure dips to avoid wasting energy. There is no heat transmission between the fluid and its surroundings in the adiabatic process. The heat is kept out of the system.

4.4 Multistage Compression

Compression in stages Air compression in multiple stages can be used to control power requirement. To make the compression less adiabatic and more isothermal, the pressurized air must be cooled between stages. Partially condensed air is typically produced by inter-stage coolers, which is removed using vapor-liquid separators. The compression curve becomes almost isothermal when the compressed air is cooled between stages. If the compressor is multi-staged, it does less work. A multi-stage compressor has a number of cylinders of different sizes. In the first phase, the air is compressed before being routed through a cooler to obtain a temp that is close to the surrounding atmosphere. The cooled air is directed to the intermediate phase, which compresses and heats it up. This air is passed through a chiller once more to bring it as near to the surrounding temperature as feasible. This pressurized air is fed into the air compressor's third

the surrounding atmosphere. The cooled air is directed to the intermediate phase, which compresses and heats it up. This air is passed through a chiller once more to bring it as near to the surrounding temperature as feasible. After cooling in an after-cooler, the compressed air is routed to the air compressor's third phase, in which it is compressed to the necessary pressure before being sent to the air receiver. Single-stage compression consumes the greatest energy, whereas multistage compression consumes the least. A multi-stage compressor is made up of numerous different sized cylinders. In the first step, the air is compressed before being routed through a cooler to reach a temperature near to that of the surrounding environment. The compressed and heated intermediate phase is pushed into the cooled air. This air is then chilled to bring it as near as feasible to the ambient temperature.

4.5 FUTURE SCOPE

Because of the fast expansion of an air-powered vehicle on the road, its aerodynamics are influenced however, if we construct a vehicle that uses that air and delivers it to an air compressor and then to an air engine, the car will not need to stop for refueling.

CHAPTER FIVE RECENT STUDIES

Some compressed air engine evaluations and experimental analyses, such as emission characteristics, compressed air power generation, compressed air power engine RPM, and, last but not least, compressed air power engine load, have been researched. Ulf Bossel's Study may not be the first of its kind, but it certainly needs to be improved. Heat exchange thermodynamics, mechanical and aerodynamic losses, electrical efficiency, and other aspects must all be taken into account. All of these factors could bring total efficiency down to 40% or below. Air vehicles, on the other hand, may have a variety of advantages in terms of system and operational costs, including simplicity, low cost, independence, zero emissions, and environmental friendliness of all system components..

Electric cars have an efficiency of 80% from battery to wheel, according to a research by S.S. According to S.S. Thipse's research, electric cars have an efficiency of 80% from battery to wheel. When an ICE with a 40% efficiency drives the air compressor, the overall efficiency of the air vehicle from fuel to wheel is $40\% \times 40\% = 16\%$, which is inefficient when compared to an IC engine or a battery-electric powertrain. The little piston in an air engine utilizes a standard connecting rod to move the crankshaft, while the bigger piston employs a new rocker arm arrangement with the connecting rod, according to Chetan K. Tembhurkar et al. This design allows the massive piston to come to a complete stop at top-dead-centre for 70 degrees of crankshaft rotation, while measured air pressure builds in a pre-chamber as the tiny piston keeps the crank spinning during its power stroke. The massive piston moves the crankshaft with increased force as the two combine to create power over 270 degrees of crankshaft rotation. On level highways, prototype air vehicles have a top speed of about 70 mph and a range of about 125 miles before requiring recharging.

Compressed air is kept in carbon fibre tanks positioned longitudinally beneath the vehicle floor at 300 bar (4351 psi). Refueling can take as little as a few minutes with a high-pressure pump or as long as four hours with a home refueling device or even an on-board compressor.

A control system was developed by Zhenggang Xu et al to lower the exhaust pressure of a vehicle compressed air driven engine. A controller, a pressure sensor, a photoelectric encoder, an intake solenoid valve, and an exhaust solenoid valve make up the control system.

The controller takes the compressed air pressure signal from the pressure sensor and the photoelectric encoder's crank angle signal, determines when the solenoid valves should open or close, and sends control signals to the solenoid valves.

According to Prof. B. S. PATEL et al, the technique is as simple as converting any ordinary IC motor vehicle's engine into an Air Powered Engine. The Air Powered Engine technology is less expensive to operate and maintain, is easily adaptable by the general public, and does not affect the environment. Rather, broad adoption will aid humanity in addressing the urgent challenge of global warming. According to a research by Bharat Raj Singh et al, global excessive hydrocarbon fuel use in the transportation sector poses a severe danger to civilization owing to future fuel scarcity. In addition, the increased use of automobiles for transportation is responsible for around 70% of overall air pollution, as well as environmental and ecological imbalances.

Employed in combination with regenerative braking. If input pressure is substantially higher than environment pressure, there is a large expansion ratio to obtain the maximum usable work to signal expansion system, according to Qihui Yu et al. As a result, two-stage expansion systems are required. In a two-stage expansion system, each stage expansion ratio is changed in order to achieve maximum output work. The production of usable work was greatly impacted by the expansion ratio of the initial stage of the system. If the first stage expansion ratio is equal to the second stage expansion ratio, the second stage expansion ratio will grow larger. To get a higher energy density, the pressure in the gas tank is high. To get the most valuable job, we should adopt a multi-stage system. The first stage expansion should be enhanced as much as feasible to two stage expansion systems in order to improve the production of valuable work.

The research of Bharat Raj Singh et al focuses on the analysis of several energy storage and conversion technologies.

The utilization of compressed atmospheric air as a feasible alternative energy source is given special attention. This type of energy storage device may be utilized as a clean energy source with no emissions, so assisting in the reduction of global warming. The revolutionary compressed air engine's performance efficiency ranges from 72 to 97 percent, making it appropriate for running a motorcycle's air engine with zero pollution. According to Mistry Manish K et al , alternative fuel or energy is necessary to meet the demand. However, while considering alternative fuels, various variables must be addressed, such as availability, cost, and environmental friendliness, among others. Based on this, CAT (Compressed Air Technology) is the best technology for reducing pollution in engines. CAE efficiency might be improved further if stress analysis, thermodynamic analysis, and minimizing compressed energy loss and other losses are carried out.

According to Rahul Kumar et al, increasing intake pressure improves average output torque and rotational speed. With the same intake pressure, the average output torque increases as the cylinder bore grows. However, when the rotational speed increases, the rotational speed decreases. The findings of this study will be useful as a starting point for additional research into design optimization.

The expansion and exhaust of air occurs within a single stroke, according to Abhishek Lal et al, making it a single stroke engine. It has a higher power output than any other compressed air engine. The work rate of a one stroke engine is considerable. The exhaust gas, which is air, is clean and cold (5 degrees Celsius). It is possible to manufacture a light-weight engine. Compressed air cars are not costly, according to Anirudh Addala et al. Compressed air cars are inexpensive and have a power-to-weight ratio of 0.0373kW/kg. The engine was changed from a 4-stroke to a 2-stroke engine utilizing a cam system operated by a crankshaft, and the intake and exhaust valves had a tiny lift as a result of this alteration, according to Chih-Yung Huang et al. At 9 pressure and 1320 rpm, the greatest power output of 0.95 kW was achieved. At the same pressure, but at 465 rpm, the greatest torque of 9.99 Nm was recorded.

The outlet pressure grew from 1.5 bar at 500 rpm to 2.25 bar at 2000 rpm, demonstrating the possibility of repurposing compressed air energy by adding more cylinders (split-cycle engine).

Dein Shaw et al used a hydraulic system powered by compressed air to show that it can surpass a pneumatic motor in terms of efficiency. The operating pressure is the most important characteristic of efficiency in a constant pressure operation; efficiency improves with reduced pressure. The residual pressure is a major factor when the air expands in the converter. Reduced air intake allows more heat to flow from the environment into the converter, increasing efficiency.

The methodology described in this paper may be used to assess the efficiency of the air/oil conversion. Between the theoretical and experimental system efficiency, there is only a 3%–3.4% discrepancy, indicating that the approach is feasible for estimating efficiency. The engine was successfully tested at two pressures, according to Naveen Kumar et al. At a lower 10 bar, a two-way NC solenoid valve with a lesser capacity (max. 10 bar) and a higher 25 bar, a three-way NC solenoid valve with a greater capacity (max. 30 bar). Both valves had a delay of roughly 20 milliseconds.

According to S. S. Verma et al., compressed air storage (both initially and during the voyage) must be controlled in a much more regulated manner, with all of the benefits of minimal heating, high energy density, and provisions to use cooling produced during adiabatic expansion during energy release. Compressed air vehicles face a serious competition from electric cars and motorcycles, not just in terms of cost but also in terms of environmental impact. Even though the technology appears to be a long way off, innovators are continuously working on it.

CHAPTER SIX RESULT AND DISCUSSION

6.1 Analysis

A 4-stroke engine is used for testing in this compressed air engine project. To convert the 4-stroke engine to a 2-stroke engine, the camshaft was adjusted. This means that one power stroke equals one complete crankshaft revolution. The atmosphere has lots of oxygen.

• According to ideal gas equation $PV=nRT$

Where,

P = Pressure

V = Volume

N = No. of moles

R = Universal Gas constant

T = Temperature

n, R, and T are commonly assumed to be constants in the preceding equation. As the equation above shows, volume is inversely related to pressure. The pressure of any gas rises as its volume decreases. This means that when air is compressed into a smaller volume, its pressure rises. As a result, a large amount of energy is stored in air as pressure energy.

When compressed air expands, it liberates energy that can be used. We learned that compressed air may readily replace other fuels after reading and studying about it. It is also stronger than gasoline. The benefits of utilizing compressed air in engines are theoretically understood, but many studies are undertaken to validate them. As a result, investigations are carried out by delivering compressed air into the engine at various pressures and recording the associated crank shaft rpm. Tests on engine performance are carried out, as well as the compressed air's effects on engine components. The following are the results of the engine tests::

At Constant Pressure

a) Experiment 1

Readings of Engine Running on compressed air at Constant pressure.

S.No.	Pressure (bar)	RPM		Mean RPM
		Min.	Max.	
1.	2	245	255	250
2.	3	455	465	460
3.	4	565	575	570
4.	5	710	720	715
5.	6	895	905	900

Running the engine on compressed air keeping the Pressure constant

Experiment #2

S.No.	Pressure (bar)	Time (sec)
1.	2	670
2.	3	425
3.	4	332
4.	5	207
5.	6	162

Run the engine on a 160-liter compressed air-filled cylinder and record the time it takes at various pressures.

Compressed air, as previously stated, can be used to replace other fuels. Because an air compressor suctions air from the atmosphere and compresses it, we converted a 4-stroke motor to a 2-stroke. As a result, the engine does not require separate suction and compression strokes. The compressed air expands and releases the energy contained in the compressed air as it is pumped into the engine, pushing the piston from TDC to BDC. The power stroke is now complete. The cold air is then ejected into the atmosphere when the piston advances from BDC to TDC.

2 stroke cycles, rather than 4 stroke cycles, are more compatible with compressed air as a fuel.

- According to the initial test When we changed the pressure and recorded the accompanying RPM, we noticed that as the pressure increased, the RPM increased as well.
- The second experiment revealed that We timed how long it took to empty the dishwasher.

With a 160 litre capacity cylinder and various pressures, we discovered that the time it takes for the cylinder to empty lowers as the pressure increases. We can assume 3 bar as the appropriate pressure for running the compressed air engine to achieve ideal RPM based on the aforementioned experiments. We got 5000 RPM at 10 bar pressure, which is enough to propel the car at roughly 100 km/hr. We can improve the engine's efficiency and use it to drive vehicles by making certain improvements to it. We can minimize the overall weight of the vehicle and engine by replacing steel parts with carbon fiber and aluminum alloys.

There are always some advantages and disadvantages to a new technology. This will also have, so let's go through each one briefly. In many aspects, compressed-air cars are similar to electric vehicles, but instead of batteries, compressed air is used to store energy.

•Like electric vehicles, air propelled vehicles would eventually be powered by the electrical grid, making it easier to focus on lowering pollution from a single source rather than the millions of vehicles on the road.

- Because the fuel would be drawn from the electrical grid, no transportation would be required. This has huge financial advantages. Pollution caused by the transportation of gasoline would be eliminated.

- Because no cooling system, fuel tank, ignition system, or silencers are required, compressed-air technology saves vehicle production costs by around 20%.

- Air is non-flammable on its own.

- The engine's size can be drastically lowered.

- Because the engine works on cold or warm air, it can be made of low-strength, light-weight materials like aluminum, plastic, or low-friction Teflon, or a mix of these materials..

- Low production and maintenance costs, as well as simple upkeep.

- Compressed-air tanks emit less pollutants when disposed of or recycled than batteries.

- Compressed-air cars are not limited by the degrading issues that plague today's battery systems.

- Lighter cars cause less damage to roads, resulting in cheaper maintenance costs.

- Airtankscanberefilledmoreoftenandinlesstimethanbatteriescanberecharged, with re-filling rates comparable to liquid fuels.

Refueling the compressed-air container with a home or low-end conventional air compressor can take up to 4 hours, whereas service stations' specialized equipment can fill the tanks in as little as 3 minutes.

CONCLUSION

This project proposed a secure mechanical system of car that utilizes the natural atmospheric air to operate. Compressed air as a fuel produce zero pollution to surrounding environment and lower the manufacturing expanses as some mechanism and not required e.g. cooling system, starter motor etc. Therefore, we can confidently say that the objectives of our program has been fulfilled successfully. However, the limited air storage and pressure capacity, and lack of reverse gearbox are the major issues associated to this transportation mean. Moreover, some experimental studies of this type of vehicles in real situation along with their results and findings was presented. Lastly, the most recently improvement and advancement of compressed air vehicles and their possible alteration stated.

references

- (1) Daniel A. Vallero, Fundamentals of Air Pollution, 5th Ed.
- (2) Kenneth Wark-Cecil F. Warner-Wayne T. Davis, Air Pollution: its origin and control, 3rd Ed.
- (3) Aqib Mehmood – Hazrat Bilal , Design Simulation and Fabrication of Vehicle Exhaust Gas Emission Control System (Smart Exhaust Technology)
- (4) Bolaji and S.B. Adejuyigbe, VEHICLE EMISSIONS AND THEIR EFFECTS ON NATURAL ENVIRONMENT – A REVIEW , Journal of the Ghana Institution of Engineers Vol. 4, No.1, 2006, pp 35–41
- (5) Ioannis Manisalidis, Elisavet Stavropoulou, Agathangelos Stavropoulos and Eugenia Bezirtzoglou , Environmental and Health Impacts of Air Pollution: A Review
- (6) Website : www.ijsrp.org/research-paper-0717/ijsrp-p6747.pdf
- (7) Website : www.sciencedirect.com/science/article/pii/S2351978920309446
- (8) Website www.sciencedirect.com/science/article/pii/S187770581400890X
- (9) JDSII , Remote Controlled Pneumatic Cylinder
- (10) Website: <https://community.createlabz.com/knowledgebase/wireless-control-nrf24101-of-servo-motors-using-joystick-module/>
- (11) Muslim Ali, Design of the Crankshaft, researchgate.net , May 2020
- (12) D. CHANAKYA GUPTA, CHAITANYA JOSHI, B RAMAKRISHNA, DESIGN AND ANALYSIS OF CRANK SHAFT , INTERNATIONAL JOURNAL OF PROFESSIONAL ENGINEERING STUDIES, Volume VIII /Issue 5 / AUG 2017
- (13) Muslim Ali, Design of connecting rod, researchgate.net , May 2020
- (14) Richard G. Budynas, J. Keith Nisbett, Shigley’s Mechanical Engineering Design, 10th Ed.
- (15) Sullivan, M. World's First Air-Powered Car: Zero Emissions by Next Summer, Popular Mechanics http://www.popularmechanics.com/automotive/new_cars/4217016.html (June 2014).
- (16) Compressed air energy storage calculations: <http://www.tribology-abc.com/abc/thermodynamics.htm> (assessed November 2012)
- (17) https://globaljournals.org/GJRE_Volume13/2-Latest-Developments-of-a-Compressed-Air.pdf
- (18) <https://www.ijert.org/research/recent-developments-of-a-compressed-air-technology-in-the-vehicles-a-review-IJERTCONV3IS17027.pdf>.